공학석사학위논문

Validity Analysis of the Performance Assessment Guideline for Existing Concrete Bridges

공용중인 콘크리트 교량의 성능평가 방법 타당성 분석

2019년 2월

서울대학교 대학원

건설환경공학부

김 민 영

Abstract

Validity Analysis of the Performance Assessment Guideline for Existing Concrete Bridges

KIM MINYEONG
Department of Civil and Environmental Enginnering
The Graduate School
Seoul National University

With economic growth, bridge constructions have been increased since the middle of the 1980s. Since the majority of bridges in Korea is concrete, especially, demand for the accurate performance assessment of an existing concrete bridge is increasing. For a deteriorated concrete bridge, deterioration, which are not seen on the exterior such as reinforcing steel corrosion caused by chloride attack or carbonation, is propagated. Accordingly, techniques to evaluate and predict such conditions and safety are required to be investigated.

As Special Act on the Control of Public Structures has been enacted in 1995, a safety inspection and an examination have been conducted for Class I and II establishments. An inspection or an examination for an existing bridge is performed according to *Detailed Guidelines for Safety Control and Maintenance of Establishments*

However, the question of whether it can evaluate an exact safety or condition

or not has been brought out continuously. Accordingly, researches associated with the question have been carried out recently. As a result, A guideline for a performance-based assessment was investigated and has been adopted since 2018 for an economic evaluation of a bridge. Nonetheless, it is controversial in a respect that the inspection items and methods are not different as the pre-existing guideline specifies.

As part of the studies, the thesis has aimed to validate the performance assessment guideline for an existing concrete bridge. To achieve this, domestic and foreign guidelines for evaluating an existing concrete bridges were examined; they were *Detailed Guidelines for Safety Control and Maintenance of Establishments* of Korea; *The Manual for Bridge Evaluation* of American Association of State Highway and Transportation Officials (AASHTO); *Code Requirements for Assessment, Repair, and Rehabilitation of Existing Concrete Structures (ACI 562-16)* of American Concrete Institute (ACI); and *BD 21/01 The Assessment of Highway Bridges and Structures* of United Kingdom. In addition, *Reliability-Based Safety Assessment Guidelines of Expressway Bridges* which was developed by Korea Expressway Corporation Research Institute (KECRI), though it has not been used as a current standard, was covered.

The study has identified that an inspection will be an inefficient task because only the domestic guideline specifies mandatory inspection items and the ways of rating each inspection results, rating in a component's level, and in a structural level. The thesis has also shown that the load rating method of the domestic guideline adopts load factors which are based on the design code of the past, and larger than the ones foreign guideline adopting. Accordingly, it has been analyzed that the guideline will evaluate a bridge conservatively. Moreover, a diagnostic load test has been pointed out as one of the problems.

Validity analyses were conducted on actual cases. Inspection reports and

relevant documents of bridges and flyovers in Seoul were collected. For each case, load rating was conducted according to every guideline examined in the study. The diagnostic load test was conducted on one of the cases. In addition, records of material test results are investigated. The investigation of load rating has shown that the domestic guideline evaluates the safety of a bridge in the most conservative way. Accordingly, it is desirable to adopt a reliability-based evaluation guideline such as AASHTO and KECRI developed. Analyzing the diagnostic test results, the study has found that the stiffness change of a structure may not be evaluated through the test. The examination of material test has confirmed that inconsistencies have been presented through the current inspections, and the study has suggested improvements for the problems.

In the further research, it is expected that the current performance assessment guideline will be improved by experimental verification of the problems presented in the thesis.

Keywords: concrete bridge, performance assessment, safety, load rating, diagnostic load test, material test, maintenance, deterioration

Student Number: 2017-29357

Table of Contents

List of Tables

List of Figures

Chapter 1 Introduction

1.1 Research Background

With economic growth, it is inevitable that most infrastructures are getting older and deteriorated. Accordingly, costs for maintenance, such as assessment, repair, rehabilitation, and deactivation are increasing. For South Korea, especially, as her economy had grown steeply in the late 20th century, the majority of infrastructures was constructed between 1980 and 2000. In Korea, since a structure is said to be deteriorated when its age is over 30, a cost for operating the infrastructure will increase after a few years.

Figure 1.1 and Table 1.1 show the statistical data of bridges built in South Korea, whose data are retrieved from KICT (2018). According to these, about 80% bridges in Korea are concrete, and 50% of them were built before the year 2000. Among them, 42% will be aged over 30 in the next 10 years, while only

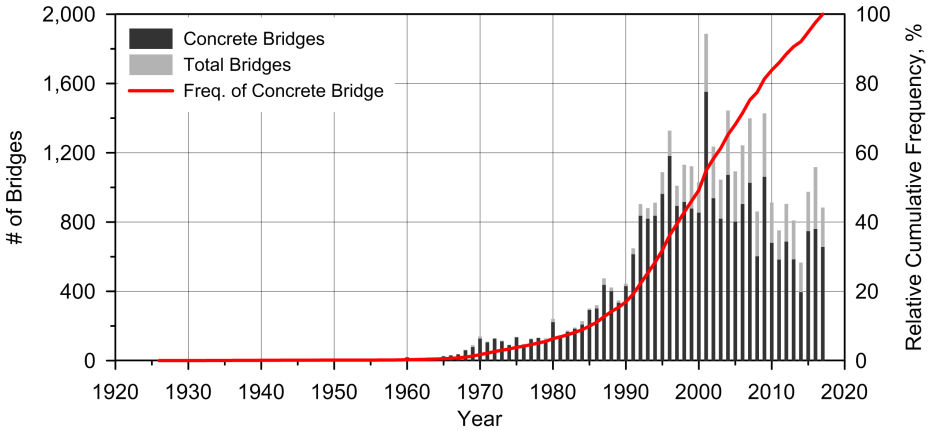

Figure 1.1: The number of bridges built in South Korea from 1926 to 2018

Table 1.1: The number of concrete bridges and their types built in South Korea from 1926 to 2018

Year	Total Bridge	Concrete Bridge	Type	Frequency
~ 1930	4	4	RC Slab	8,255
1930~ 1940	18	14	RC T Beam	760
1940~ 1950	21	21	RC Hollow Slab	237
1950~ 1960	19	16	RC Box	214
1960~ 1970	331	298	Rhamen	7,859
1970~ 1980	1,207	1,157	PSC I Beam	7,546
1980~ 1990	2,846	2,685	PSC Box	631
1990~ 2000	9,470	8,365	PSC Slab	476
2000~ 2010	12,666	9,629	PSC Hollow Slab	37
2010~	6,921	5,092	Pre-flex	1,332
Total	**33,503**	**27,281**	**Total**	**27,281**

14% are aged over 30 currently. Moreover, considering the budget on road system of Korea as in Figure 1.2, the budget on road maintenance tendency of increasing; the fraction of maintenance tends to increase while that of construction tend to decrease (KICT, 2017; MOLIT, 2016a). Accordingly, the maintenance cost of an existing concrete bridge would be increased considerably in near future; the demand for the efficient assessment of the bridge is increasing for the efficient operation of the bridge.

1.1.1 Performance Assessment in South Korea

In early 1990s Korea, two cases of severe accidents occurred. What caused these accidents were structural deficiencies, which had not been detected. To avoid such accidents, the government legislated a law, Special Act on the Safety Control of Public Structures (1995) and a guideline (KISTEC, 1995). According

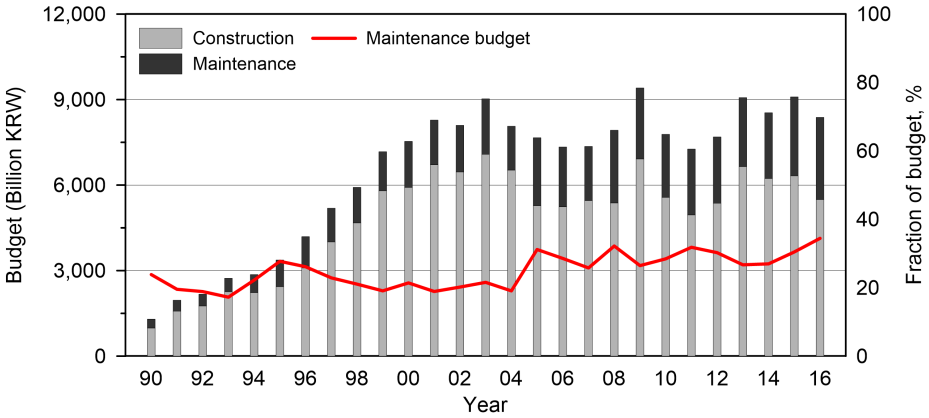

Figure 1.2: Budget on road construction and maintenance in South Korea from 1990 to 2016

to the law and the guideline, safety evaluations (or assessments) are conducted regularly on infrastructures.

According to the law and its enforcement ordinance (KISTEC, 2018b), establishments in Korea are categorized into three classes. A highway bridge, especially, is classified as table 1.2. Types of assessments conducted to a bridge are different according to the class of a structure; their conducting cycles are different from each other according to the grade of an establishment. The types and their intervals are summarized in Table 1.3.

The procedures are summarized in Figures 1.3, 1.4 and 1.5 (KISTEC, 2018b). In the periodic safety inspection (Figure 1.3), visual inspection is mainly conducted focusing on what precedent assessment have observed. Then, the current exterior condition is compared with the past one.

The full safety inspection (Figure 1.4) and the examination (Figure 1.5) comprise the conditional and the structural safety evaluation. In the full safety inspection, only conditional safety of major component is evaluated; in a full safety examination, both conditional and structural safety of the whole com-

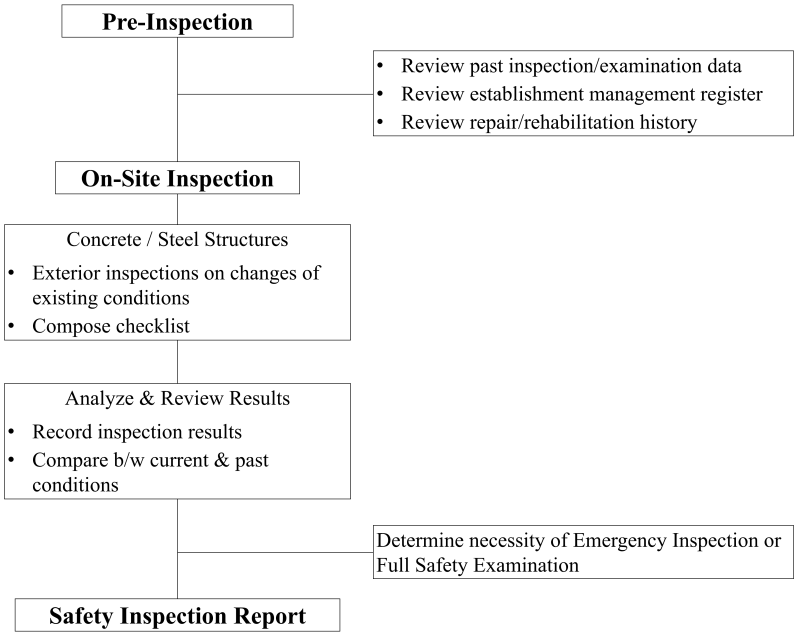

Figure 1.3: The procedure and content of a periodic safety inspection

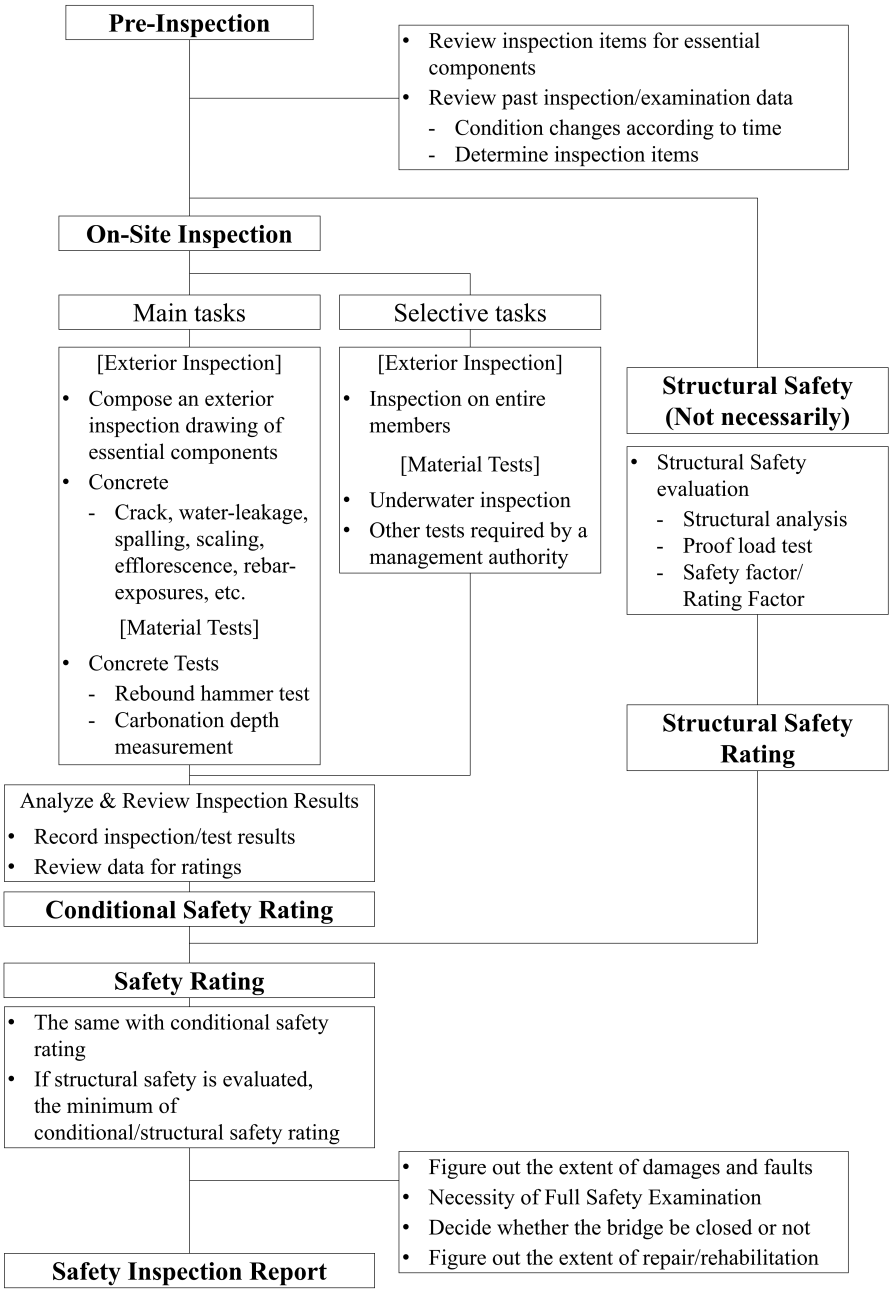

Figure 1.4: The procedure and content of a full safety inspection

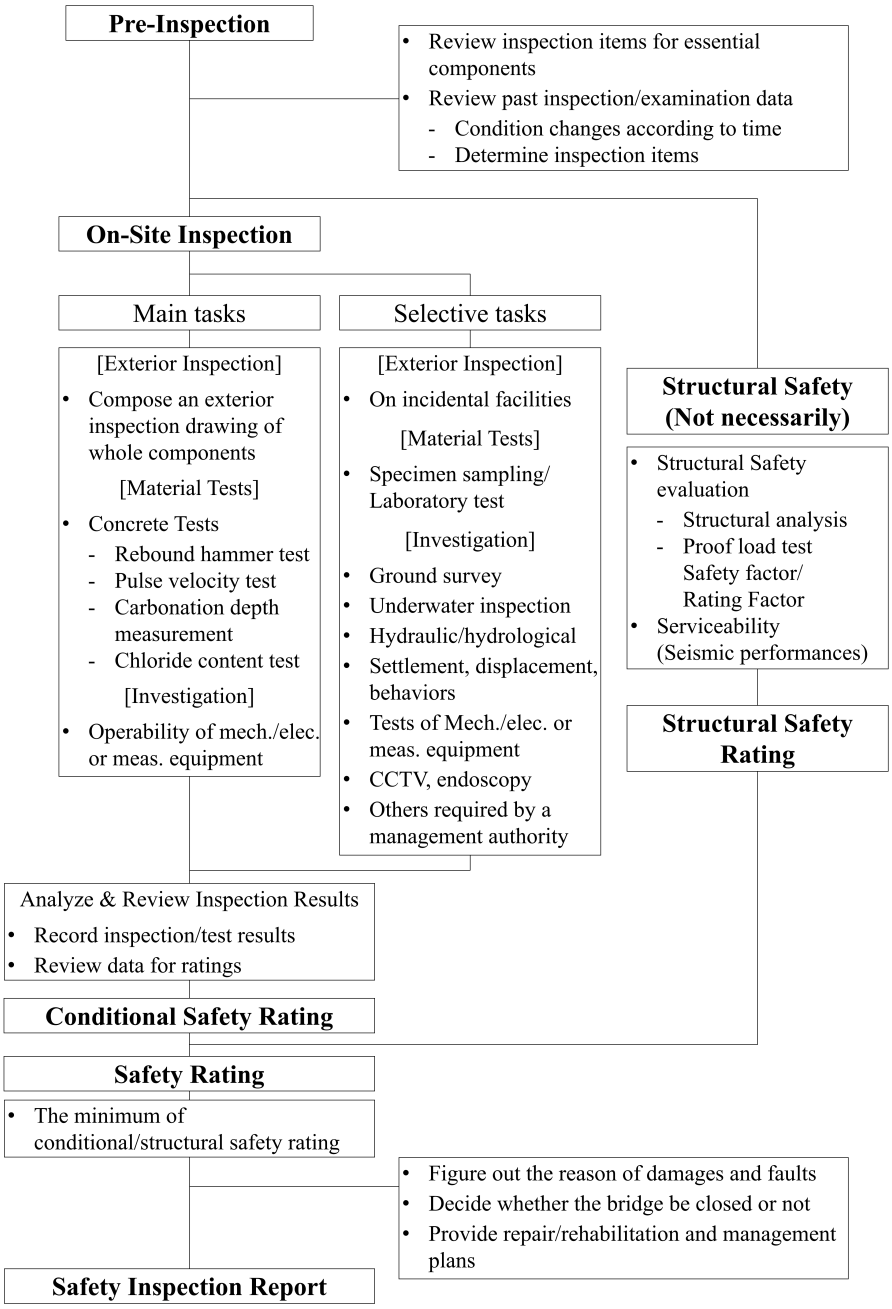

Figure 1.5: The procedure and content of a full safety examination

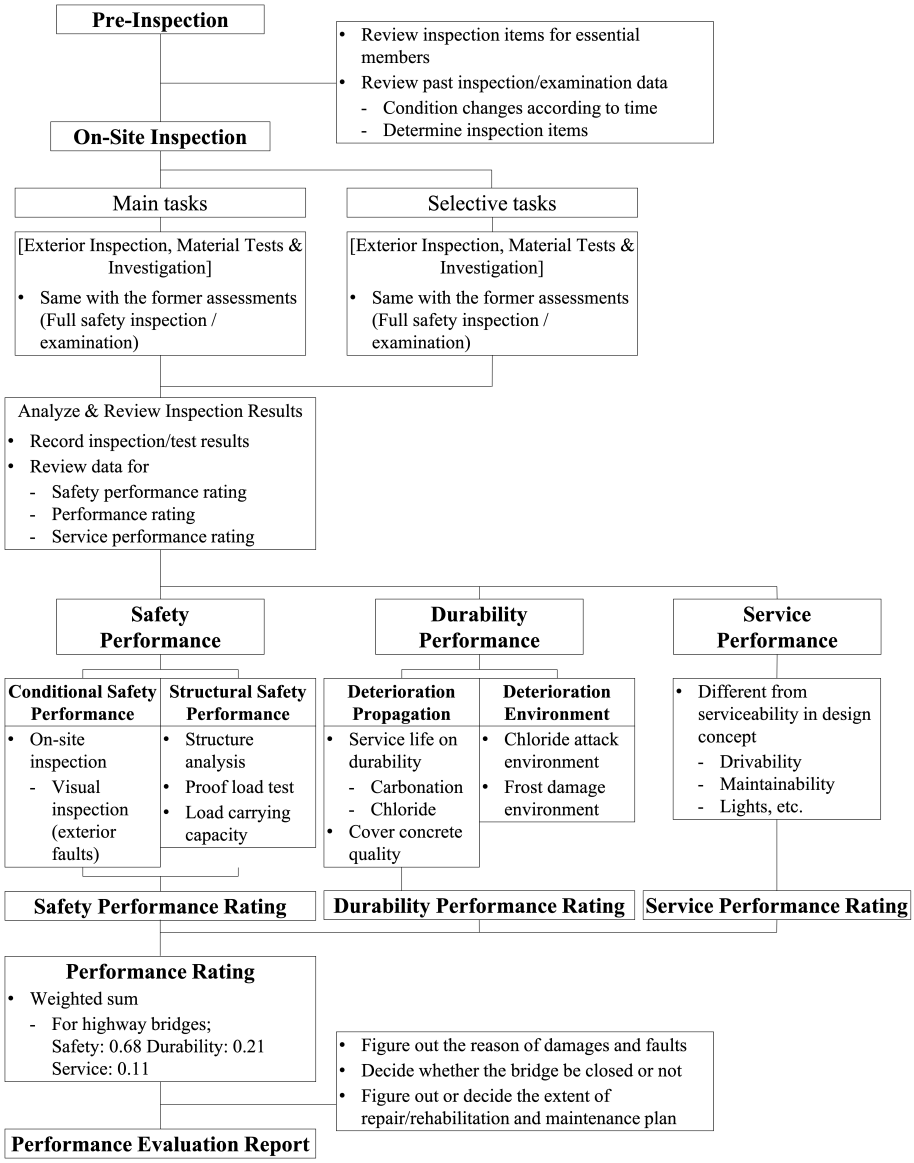

Figure 1.6: The procedure and content of a performance evaluation

ponents are obligatorily evaluated. Here, conditional safety is determined by on-site inspection and material tests. Structural safety is determined by a load rating procedure. The safety rating of an establishment is represented by one grade between 'A' and 'E'.

Since 2018, KISTEC (2018a) has been legislated for an efficient assessment of existing establishment. Its procedure and content are as shown in Figure 1.6.

The safety performance is the same procedure with the pre-existing guideline, except that the evaluations of material tests are excluded. Instead, the tests are considered in the durability performance evaluation. The deterioration environment of the durability procedure is evaluated using statistical data such as weather or location from a coastline, however, it is not used to determine the overall durability performance. Additionally, rating about the facilities is newly prescribed as the service performance evaluation. Here, the term service is not the serviceability in design. The overall performance rating is determined by weight-summing the three performances.

Table 1.2: The classification of highway bridge in Korea

<table>
<tr><th>Class I</th><th>Class II</th><th>Class III</th></tr>
<tr><td>Maximum span length over 50 m</td><td>Single span bridge with $L \geq 50$ m</td><td rowspan="4">Age over 10 with $L \geq 20$ m,
- regulated by Road Act and $L < 100$ m
- regulated by Act on the Maintenance and Improvement of Road Networks in Agricultural and Fishing Village
- not regulated</td></tr>
<tr><td>$L \geq 500$ m</td><td>$L \geq 100$ m and $L < 500$ m</td></tr>
<tr><td>Covered structure with width over 12 m and $L \geq 500$ m</td><td>Covered structure with width over 6 m and $L \geq 100$ m</td></tr>
<tr><td>Cable-stayed, Suspension, Arch, or Truss Bridge</td><td>-</td></tr>
</table>

Table 1.3: The classification of highway bridge safety inspections in Korea

	Periodic Safety Inspection	**Full Safety Inspection**	**Full Safety Examination**
Mandatory for	Class I, II & III Establishment	Class I & II Establishment	Class I Establishment
Cycle time	A, B, C: < 0.5 yr D, E: < 1/3 yr	A: < 3 yr B, C: < 2 yr D, E: < 1 yr	A: < 6 yr B, C: < 5 yr D, E: < 4 yr

The thesis has used a term 'performance assessment' to represent every inspection type. The detailed criteria are taken into account in clause 2.1.

1.1.2 Limitations on Performance Assessment in South Korea

The procedure of the current assessment (full safety inspection or examination) is summarized as Figure 1.7. The procedure is categorized into the conditional and structural safety evaluation. However, there are some limitations.

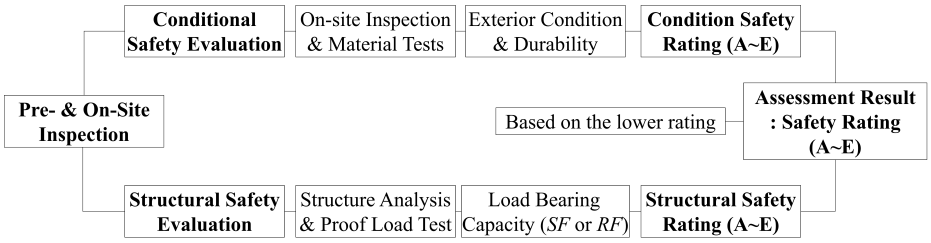

Figure 1.7: The schematic diagram of bridge inspection in Korea

First, assessing methodologies have limitations. KISTEC (2018b) suggests the item of visual inspection; for a concrete component, crack, spalling, scaling, efflorescence, water leakage or exposure of reinforcing steel are examined; for a supplementary component, such as a viaduct, a joint or a shoe, etc., some damages or existences of sediments are examined. Since they are observed on

the exterior with naked eyes, the interior condition cannot be evaluated. Moreover, these exterior faults do not represent the global phenomena. For instance, an extensive rebar exposure caused by corrosion rarely occurs for concrete in a moderate environment. In other words, the widespread existences of such faults will occur in a severe environment, such as a splash zone. Plus, the interaction between such local faults and a global behavior is not clear. Consequently, it might be said that the inspection does not reflect the actual condition.

In the same manner, most faults of the bridges investigated by the tests are the local ones caused by deicing salt or general deterioration as being operated. Hence, the items of material tests might not be proper to implement regardless of a structure's characteristic.

Evaluating the structural safety of an existing bridge should be based on the current condition of damage and deterioration. The guideline states that, since it is difficult to quantify their extents, when determining a nominal strength, only the change of a cross-section or a material strength needs to be considered while using the resistance factor of design criteria (KISTEC, 2018a; 2018b). However,

Table 1.4: Examples of safety rating for real concrete bridge cases

Cases (Evaluated Year)	**Built Year**	**Conditional Safety**	**Structural Safety**	**Safety Rating**
A Bridge (2011)	1968	**C**	A	**C**
J Bridge (2012)	1978	**C**	B	**C**
W Bridge (2012)	1986	**B**	A	**B**
H Bridge (2013)	1976	**B**	A	**B**

Table 1.5: The rating system specified in Detailed Guidelines for Safety Control and Maintenance of Establishments

Rating	Safety of an Establishment
A	The best condition without any fault
B	The condition of minor faults on supplementary components without affecting functionality; they require to be partly repaired to enhance durability
C	The condition of minor faults on essential components or extensive faults on supplementary components without affecting the safety of establishment; the essential component requires to be repaired; the supplementary component requires to be partly strengthened to prevent fall of durability and functionality
D	The condition of faults on essential components; they require to be emergency repaired and strengthened determining whether being closed or not
E	The condition of extensive faults on essential components with threatening the safety of establishment; the establishment requires to be closed and retrofitting or rebuilding

in a practical application, since the load rating is based on the design, it might not reflect the actual safety of a concrete bridge.

The rating based on the lower rate between conditional and structural safety seems to have a limitation. As shown in Table 1.4, most concrete bridges show the lower rate in conditional safety. Hence, the safety ratings of structures are determined mainly by conditional safety. Consequently, the safety can be underestimated by exterior faults, accordingly, their maintenance decisions can be made by such defects.

KISTEC (2018b) or KISTEC (2018a) specified the rating system of an establishment as Table 1.5 and a maintenance decision also depends on it. However, it is arguable that the safety of a bridge can be represented by one grade.

KISTEC (2018a) adopted recently for an economic and accurate assess-

ment, shares similar limitations with the former guideline. The safety performance procedure is identical with the current guideline, and the largest weight is put on the performance. Consequently, it will focus on exterior deficiencies or service performances as well.

1.1.3 Preceded Researches on Materials Deterioration Model

To find the way of estimating existing structures' performance without low efficient assessments, preceded researches about materials deterioration are investigated.

Tuutti (1980, 1982) investigated the corrosion of reinforcing bars in terms of service life. The paper suggested that the service life is divided into two stages; initiation stage when CO_2 or Cl^- penetrates to steel and; propagation stage when cover cracking begins. In the studies, a mathematical model for passive film breaking and penetrations of the causative substances are suggested.

Weyers (1998) suggested that there is a period that rust products of reinforcing steel does not exert expansive pressure after the initiation stage proposed in Tuutti (1980, 1982) While some of the products have an effect to fill entrapped air or capillary voids around steel. Also, it estimated the critical time analytically, when a crack propagates to a concrete surface, adopting Fick's law and Faraday's law.

Bhargava, Ghosh, Mori, and Ramanujam (2005); Liu and Weyers (1998); Maaddawy and Soudki (2007) investigated time-to-corrosion initiation and corrosion cracking both analytically and experimentally. They adopted the thick-walled cylinder theory of continuum mechanics, proposed models of rust production and crack propagation by time. Based on the researches, Shodja, Kiani, and Hashemian (2010) suggested a numerical nonlinear model for stress and

displacement field around a corroded reinforcing bar.

C.-Q. Li, Melchers, and Zheng (2006); Pantazopoulou and Papoulia (2001); Vidal, Castel, and Francois (2004) estimated the crack width caused by steel corrosion. They chose factors affecting the crack propagation corrosion rate, concrete geometry, and its properties. Adopting Fick's law, Faraday's law, and continuum mechanics, they proposed numerical solutions for the crack width by time. Chen and Mahadevan (2008) modeled and simulated corrosion of reinforcing bars in chloride environment with finite element analysis and thermal analysis. Molina, Alonso, and Andrade (1993) also verified the cover cracking of concrete using the finite element analysis using DIANA FEA.

Almusallam, Al-Gahtani, Aziz, and Rasheeduzzafar (1996); Auyeung, Balaguru, and Chung (2000); Lee, Noguchi, and Tomosawa (2002) verified the interaction between steel corrosion and the bond strength reduction between steel and concrete, through pullout tests or cantilever bond tests with corroded steels. They found that the bond strength increases before 4% of steel corrosion, and markedly decreases after that. Bhargava, Ghosh, Mori, and Ramanujam (2007); Castel, Khan, Francois, and Gilbert (2016) proposed models empirically and analytically, respectively, about a bond strength reduction according to the corrosion. Especially, Castel et al. (2016) investigated the confinement effect of stirrups on the bond strength. Al-Sulaimani, Kaleemullah, Basunbul, and Rasheeduzzafar (1990); Fang, Lundren, Plos, and Gylltoft (2006); Lundren (2002) verified a bond strength of corroded steel with some experiments and finite element analyses.

Andrade, Alonso, and Molina (1993); C.-Q. Li (2003) suggested limit states about steel corrosion of a concrete member and experimentally verified them. Cabrera (1996) investigated crack width, bond strength reduction, and serviceability loss caused by corrosion of reinforcement, with experiment. Also, it de-

ducted a numerical model for those phenomena.

Han, Lee, Kim, Seo, and Moon (2014) provided the procedure for numerical calculation of the flexural strength of a reinforced concrete member with corroded steels. It considered the sectional loss of a steel and a bond strength reduction due to corrosion; and a corrosion pressure, etc.

Saetta (2005) provided the approach to estimating load-bearing capacity loss using the constitutive relation of damaged concrete with regards to carbonation and steel corrosion and verified with finite element analyses and experimental results. It observed losses of ultimate strengths and ductility of a reinforced concrete slab.

Goltermann (1994a, 1994b) suggested the model of stress distribution around a deteriorated concrete caused by expansion and shrinkage; highly reactive aggregates; or their expansions using fracture mechanics. Moreover, it provided the decision tree about the cause of a crack pattern. Bangert, Kuhl, and Meschke (2004); Gao, Li, and Zhao (2013); Ichikawa and Miura (2007); Piast and Schneider (1992) investigated the influence of an alkali-silica reaction or a sulfate attack on concrete properties, its strength, and their mechanisms.

Basheer, Chidac, and Long (1996) presented the relation between various mechanisms of concrete deterioration including steel corrosion, frost damage, sulfate, and acid attack. It provided the way of determining contact pressure caused by such deterioration, following the approaches of Goltermann (1994a, 1994b).

Coronelli, Castel, Vu, and Francois (2009); Guo, Frangopol, Han, and Chen (2011); F. Li, Yuan, and Li (2011); Vu, Castel, and Francois (2009); L. Wang et al. (2014) investigated a prestressed concrete deterioration. They investigated corrosion of steel strands, in terms of uniform, pitting or stress corrosion, and

its effect on a concrete behavior.

In the precedent researches, many models and techniques for estimating and simulating concrete deterioration are proposed. However, they are focused on either service life, material level tests or ideal situations such as the uniform corrosion of steel. Also, there is no model to predict a concrete behavior as a function of time.

There exist few attempts to simulate the concrete behavior with a nonlinear finite element analysis. Nonetheless, it is difficult to adopt the techniques into structural level practically. In other words, there is no way to evaluate or estimate the safety degradation of an existing concrete bridge other than the current assessments.

1.2 Research Objectives and Scopes

The limitations of the current assessment on a concrete bridge are summarized as below:

1. The current assessments are focused on exterior conditions and there is no clear relation to the condition and actual safety;
2. The structural safety of a bridge is evaluated based on a design document;
3. The overall safety of a bridge is determined by the lower grade between conditional and structural safety; accordingly, the bridge's safety can be evaluated mainly with exterior faults;
4. The safety of a bridge is represented by one alphabet among five;
5. There is no time-dependent model to predict the current state of a concrete bridge analytically

To deal with the problems, the current performance assessment guideline for an existing concrete bridge needs to be investigated closely.

For this, domestic and foreign guidelines were compared and analyzed.

Second, case studies on existing concrete bridges were conducted. Here, the load rating method, diagnostic load test and material tests and their rating methods were verified.

Third, experimental verification needs to be conducted. Evaluating condition at the interior of a decommissioned components and conducting load test and flexural test, the assessment's validity would be examined thoroughly. However, the experimental verification has not been conducted in the thesis. The further research will cover it.

Chapter 2 Guidelines for Assessment of Existing Concrete Bridges

In the chapter, the domestic and foreign guidelines have been compared and analyzed to verify the domestic guideline. The thesis examined the following documents:

1. Detailed Guidelines for Safety Control and Maintenance of Establishments (2018);
2. AASHTO The Manual for Bridge Evaluation (2013); together with FHWA Recording and Coding Guide (1995) and Bridge Inspector's Reference Manual (2012);
3. ACI 562-16 Code Requirements for Assessment, Repair, and Rehabilitation of Existing Concrete Structures (2016);
4. BD 21/01 The Assessment of Highway Bridges and Structures (2001);
5. Reliability-Based Safety Assessment Guidelines of Expressway Bridges (2013)

Between guidelines, there was no difference in visual inspection and material tests while there were differences in load rating methods. Hence, clauses from 2.2 to 2.4 have focused on load rating methods.

2.1 Detailed Guidelines for Safety Control and Maintenance of Establishments (2018, Korea)

Detailed Guidelines for Safety Control and Maintenance of Establishment (KIS TEC, 2018a; 2018b) have been used to assess concrete bridges in Korea. Items

for assessment of a concrete bridge are categorized into on-site inspection, material test, and load rating.

2.1.1 On-Site Inspection and Material Test

In evaluating conditional safety, on-site inspections and material tests are conducted. KISTEC (2018a, 2018b) suggests the target inspection regions and damages as in Tables 2.1 to 2.3. The items in the tables are essentially inspected in every full safety inspection or examination. They are concentrated in the external damages without clarifying the causes of occurrences.

Table 2.1: Targeted inspection regions and damages for a reinforced concrete deck specified in the domestic guideline

Inspection Region		**Damages**
Commons		• crack, spalling, scaling, separation, rebar exposure • segregation • leakage, efflorescence
Beam Bridge		• crack, network cracking
Slab/Rahmen	End-span	• crushing • diagonal tensile crack
	Mid-span	• flexural crack

Table 2.2: Target inspection regions and damages for a reinforced concrete beam specified in the domestic guideline

Inspection Region	**Damages**
Commons	• spalling, scaling, separation, damage, rebar exposure, efflorescence
End-span	• crushing • diagonal tensile crack
Mid-span	• flexural crack

Table 2.3: Target inspection regions and damages for a prestressed concrete beam specified in the domestic guideline

Inspection Region		Damages
Commons		• spalling, scaling, rebar exposure, efflorescence
End-span		• crushing • web diagonal crack, flexural crack • crack on wall opening
Mid-span		• flexural crack, deflection • sheath exposure & damage • crack on flange or web in PC wire direction • crack or leakage on construction joint
Anchorage		• crack, damage
PC strands	Strand	• corrosion, rust, fracture
	Sheath	• damage, insufficient grout, rust, corrosion

Table 2.4: The criteria for conditional safety rating of a prestressed concrete girder

Rating	Girder		Tendons		
	Crack	**Damage & Corrosion**	**Exposure & Damage**	**Grouting Fault**	**Sheath Damage**
a	- none	- none	- none	- none	- none
b	- width ~ 0.2 mm	- area ~ 2%	- exposed	- fault	- damaged
c	- width 0.2 ~ 0.3 mm	- area 2 ~ 10% - corroded ~ 2%	- surface rust	- chloride content 1.2 ~ 2.5 kg/m^3	
d	- width 0.3 ~ 0.5 mm - excessive flexural crack	- area 10% or more - corroded more than 2%	- corroded with section loss	- chloride content 2.5 kg/m^3 or more	
e	- width 0.5 mm or more - excessive flexural crack and deflection	- excessive damage on end-span, damage on anchorage	- fracture		

A prestressed concrete component, for instance, is rated as Table 2.4. The inspection of a tendon is specified, however, it is concentrated on an external tendon, not an internal one. In addition, inspections on supplementary components such as a shoe, an expansion joint, a viaduct, or a barrier, are conducted.

Among material tests, carbonation depth and chloride content test are used to rate conditional safety. A concrete strength examined through a nondestructive test or a core specimen does not affect a conditional safety. Using the test results, a conditional rating is determined according to Table 2.5 and 2.6 (KISTEC, 2018b). In durability evaluation of KISTEC (2018a), material test results are evaluated according to Tables 2.7 to 2.10.

Table 2.5: The domestic guideline's criteria evaluating a condition according to carbonation depth

Rating	**Remaining Carbonation Depth**	**Possibility of Steel Corrosion**
a	30 mm or more	no concern of corrosion
b	10 mm ~ 30 mm	exists possibility of corrosion
c	0 mm ~ 10 mm	high possibility of corrosion
d	less than 0 mm	steel corrosion occurred

Table 2.6: The domestic guideline's criteria evaluating a condition according to chloride content

Rating	**Chloride Ion Content at Cover Depth**	**Possibility of Steel Corrosion**
a	0.3 kg/m^3 or less	no concern of corrosion
b	0.3 kg/m^3 ~ 1.2 kg/m^3	low possibility of corrosion
c	1.2 kg/m^3 ~ 2.5 kg/m^3	high possibility of corrosion
d	2.5 kg/m^3 or more	steel corrosion occurred

Table 2.7: The domestic guideline's criteria evaluating a durability according to carbonation depth

Rating	**Time When a Remaining Depth is Carbonated, T**	**Notes**
a	30 yrs or more	$A = \frac{D}{\sqrt{t}}$ $T = \left[\frac{\text{Cover thickness}}{A}\right]^2 - t$ A: Carbonation rate coefficient D: Carbonation depth, t: Years of use
b	20 yrs ~ 30 yrs	
c	10 yrs ~ 20 yrs	
d	5 yrs ~ 10 yrs	
e	less than 5 yrs	

Table 2.8: The criteria of the domestic guideline evaluating a durability according to chloride content

Rating	**Time When Chloride Content, C_r = 2.5 kg/m^3**	**C_r (kg/m^3)**	**Notes**
a	30 yrs or more	0.3 or less	• Determine diffusion coefficient and time to chloride content reaches the critical value • Evaluate according to the lower between the rating by the time when chloride content reaches 2.5 kg/m^3 and C_r
b	20 yrs ~ 30 yrs	0.3 ~ 0.6	
c	10 yrs ~ 20 yrs	0.6 ~ 1.2	
d	5 yrs ~ 10 yrs	1.2 ~ 2.5	
e	less than 5 yrs	2.5 or more	

Table 2.9: The domestic guideline's criteria evaluating a durability by comparing concrete strength

Rating	**The Ratio of Strength (Estimated/Design)**	**Notes**
a	1.0 or more	sound quality of cover concrete
b	0.9 ~ 1.0	durability loss begins
c	less than 0.9	durability loss progressed

Table 2.10: The domestic guideline's criteria evaluating a durability by comparing sound and unsound regions

Rating	**The Ratio of Rebound (Unsound/Sound)**	**Notes**
a	0.95 or more	no big difference compared to sound region
b	0.85 ~ 0.95	durability loss begins
c	less than 0.85	durability loss progressed

Difference between conditional safety and durability is that the former is evaluated with a test result itself while the latter is evaluated in terms of remaining service life. Also, the durability of a component can be determined by a cover concrete quality using a rebound hammer (also known as Schmidt Hammer) test result. The durability performance is evaluated by comparing a presumed concrete strength to a specified strength or by comparing rebound values between sound and unsound region are compared.

In summary, a conditional safety is determined by the rating of each inspection and material test item. The criteria are found to be deterministic from the point of view that every item is graded quantitatively according to an inspected result itself. In KISTEC (2018a), on the other hand, material test results are used

Table 2.11: Conditional deficiency score, p_n and the rating criteria according to the range of evaluated condition index, X

	A	**B**	**C**	**D**	**E**
p_n	0.10	0.20	0.40	0.70	1.00
X	0 to 0.13	0.13 to 0.26	0.26 to 0.49	0.49 to 0.79	0.79 or more

to evaluate a durability performance in less deterministic ways, which are based on service lives.

Each item is rated from a to e for every component. The lowest rating among items is set as a component's condition. Then each component is scored according to its rating according to Table 2.11. The weight-average of all components' conditions (Eq. (2.1)) is set as an establishment's condition.

$$X = \sum_n (p_n \times w_n) \tag{2.1}$$

Here, w_n refers to the weight of each component.

In the performance evaluation, p_n is replaced by X_n, the performance deficiency score; and w_n is replaced by W_n, the weight on each performance. A performance index, E is evaluated by Eq. (2.2). The rating criterion is the same with Table 2.11.

$$E = \sum_n (X_n \times W_n) \tag{2.2}$$

In the condition evaluation of a general beam bridge, for instance, w_n's are specified as follows; 0.18 on a deck; 0.20 on a girder; 0.05 on secondary components; 0.20 on a substructure; 0.09 on a shoe; 0.21 on supplementary components; and 0.07 on a carbonation condition. Shortly, 53% of weight is applied to components that are replaceable and that do not have clear correlation with a global behavior such as a deck, a shoe, or supplementary components. It implies that the conditional safety and according maintenance can be determined

by exterior faults on such replaceable components.

2.1.2 Load Rating

KISTEC (2018a, 2018b) specify the structural safety assessment based on the safety factor and the rating factor as Eqs. (2.3) and (2.4).

$$SF = \frac{f_a}{f_{d+l}} \quad \text{or} \quad \frac{\varphi M_n}{M_u} \tag{2.3}$$

$$RF = \frac{f_a - f_d}{f_l(1+i)} \quad \text{or} \quad \frac{\varphi M_n - \gamma_d M_d}{\gamma_l M_l(1+i)} \tag{2.4}$$

where,

f_a	actual strength
f_d, f_l	stresses due to dead load; and live load, respectively
f_{d+l}	required strength
i	design impact factor; $15/(40+L) \leq 0.3$, L is a span length in m
M_d, M_l	moments at section due to dead load; and live load, respectively
M_n	nominal flexural strength at section
M_u	factored moment at section
γ_d, γ_l	load factors for dead load; and live load, respectively
φ	resistance factor; for a flexural member, $\varphi = 0.85$

The rating factor stands for the ratio of a live load margin to a design live load. Here, the live load margin is the amount of a load which can be carried in addition to a dead load.

KISTEC (2018a, 2018b) specifies SF and RF based on both allowable stress and strength design approaches. A concrete bridge is evaluated by the strength design approach.

For a concrete highway bridge, load combination is $1.30D + 2.15L(1+i)$ and the resistance factor is 0.85 for flexure. The load combination is originated from MLTM (2010) which is the design code in a strength design concept. The

resistance factor of 0.85 is the commonly used factor specified in the design code of Korea such as KCI (2017); MOLIT (2016b); MLTM (2010).

In the Korean guidelines, the response compensating factor, K_s is defined as Eq. (2.5). The factor is applied to reflect a difference in response between analysis and an experiment.

$$K_s = \frac{\varepsilon_{calc}}{\varepsilon_{meas}} \times \frac{1 + i_{calc}}{1 + i_{meas}} = \frac{\delta_{calc}}{\delta_{meas}} \times \frac{1 + i_{calc}}{1 + i_{meas}} \tag{2.5}$$

where,

i_{calc}	calculated impact factor; i.e. design impact factor
i_{meas}	measured impact factor
δ_{calc}	deflection calculated by structure analysis
δ_{meas}	deflection measured by diagnostic load test
ε_{calc}	strain calculated by structure analysis
ε_{meas}	strain measured by diagnostic load test

The load carrying capacity of a structure, P is defined as Eq. (2.6). This means the permissible live load that a structure can carry within its strength. Here, the design load is DB and DL loads specified in MLTM (2010).

$$P = K_s \times RF \times P_r \tag{2.6}$$

where,

P_r	design live load specified in Table 2.12 and Figure 2.1.

The structural safety evaluation criteria are defined as Table 2.13. The safety mainly depends on the safety factor.

In summary, the structural safety of a concrete bridge is evaluated by the safety factor or the rating factor together with the response compensating factor. The load and resistance factors are identical to the design code, MLTM (2010)

Table 2.12: DB design truck load specified in Korean Highway Bridge Design Code (2010)

Designation	**Weight, W (kN)**	**Total Load, $1.8W$ (kN)**	**Front, $0.1W$ (kN)**	**Rear, $0.4W$ (kN)**
DB-24	240	432	24	96
DB-18	180	324	18	72
DB-13.5	135	243	13.5	54

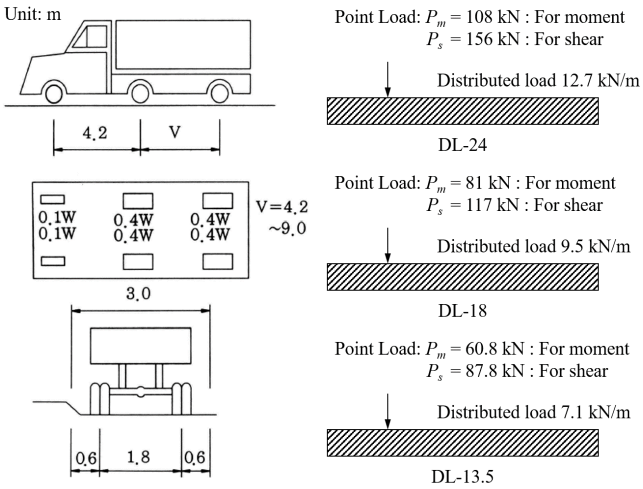

Figure 2.1: DB design truck geometry(left) and DL design lane load(right) specified in Korean Highway Bridge Design Code (2010)

which had been used until 2012. Accordingly, the main weakness is that its concept is too outdated for a practical application. It does not accept reliability method, which has been widely used in a design. Moreover, its load factors are larger than those in the current design codes; in MOLIT (2016b), 1.25 on a dead component and 1.80 on a live load; in KCI (2017), 1.2 on a dead load and 1.6 on a live load.

As discussed in the introduction, the structural safety should be evaluated

Table 2.13: The criteria to evaluate the condition in terms of the comparison between sound and unsound regions in Korean guideline

Rating	**Criteria**
A	$SF > 1.0$
B	$0.9 \leq SF < 1.0$; and load carrying capacity, P is more than the design load
C	$0.9 \leq SF < 1.0$
D	$0.75 \leq SF < 0.9$
E	$SF < 0.75$

based on the current state of a structure in principle. Nevertheless, in the practical evaluation, usually the sectional losses of materials are negligibly small, and because of the complexity of a calibration process, resistance factor in design code is used without any calibration (KISTEC, 2018a, 2018b). Therefore, a practical structural safety evaluation will be the same procedure of design with the same safety margin. In other words, an existing bridge's safety will be evaluated in a conservative manner.

Moreover, to determine response compensating factor, a diagnostic load test is conducted. In Korea, it is obligatorily conducted in a full safety examination though it is an expensive and time-consuming process. The limitations were closely covered in the following chapter.

2.2 AASHTO The Manual for Bridge Evaluation (2013, US)

In the Federal Regular, National Bridge Inspection Standards (2009) regulates the safety inspection of an existing highway bridge in the United States. In §650.317, American Association of State Highway and Transportation Officials(AASHTO) The Manual for Bridge Evaluation (AASHTO, 2013) is referenced as a single guideline for assessing the bridge. Hereafter, it is abbreviated to AASHTO MBE.

The inspection items are similar to the domestic guideline. However, it does not specify the way of rating a result as a grade. It covers the way of reporting an inspection result and recommends tasks not regulating them. The rating method is specified in FHWA guide (FHWA, 1995), it is covered in the clause 2.2.2.

2.2.1 Load Rating

The objective of the load rating in AASHTO MBE is to evaluate a general highway bridge under a permanent load and a vehicle load in the United States; an extreme load such as an earthquake, wind or a collision is not considered.

The load rating comprises two approaches; load and resistance factor rating (LRFR); allowable stress rating (ASR) and load factor rating (LFR). LRFR is the approach which adopts the concept of load and resistance factor design (LRFD), currently used in the design of a U.S. highway bridge (AASHTO, 2017). Besides, ASR or LFR approach is based on the former design specification of U.S. (AASHTO, 2002)

The LRFR Approach

The rating factor of the LRFR approach is defined as Eq. (2.7).

$$RF = \frac{C - (\gamma_{DC})(DC) - (\gamma_{DW})(DW) \pm (\gamma_P)(P)}{(\gamma_{LL})(LL + IM)} \tag{2.7}$$

where,

C	Capacity
	= $\varphi_c \varphi_s \varphi R_n$, for the strength limit state; $(\varphi_c \varphi_s \geq 0.85)$
	= f_R, for the service limit state
f_R	allowable stress specified in the LRFD code
R_n	nominal member resistance (as inspected)
DC	dead load effect due to structural components and attachments
DW	dead load effect due to wearing surface and utilities
P	permanent loads other than dead loads
LL	live load effect
IM	dynamic load allowance as specified at clause 3.6.2 of the LRFD code
γ_i	according load factors as specified in Table 2.16
φ_c	condition factor as specified in Table 2.14
φ_s	system factor as specified in Table 2.15
φ	LRFD resistance factor

In LRFR, the capacity of a structure, C is defined as above. In addition to a nominal strength and a resistance factor of the design code, the condition factor, φ_c and the system factor, φ_s are applied. The former reflects a strength loss due to deterioration which is not considered in computing R_n; the criterion for determining φ_c is as Table 2.14. The latter reflects the redundancy of a bridge superstructure so that the system reliability of a non-redundant system can be

Table 2.14: Condition factor, φ_c according to the LRFR approach of AASHTO MBE

Condition of a Member	**Condition Factor, φ_c**
Good or Satisfactory	1.00
Fair	0.95
Poor	0.85

Table 2.15: System factor for a concrete bridge resisting bending or axial force, φ_s according to the LRFR approach of AASHTO MBE

Superstructure Type	**System Factor, φ_s**
Three-Girder Bridges with Girder Spacing 6 ft	0.85
Four-Girder Bridges with Girder Spacing≤4 ft	0.95
All Other Girder Bridges and Slab Bridges	1.00

increased. For a member resisting bending or axial force, AASHTO (2013) recommends it as Table 2.15. The values are conservative than the LRFD values and may be used at the discretion of the evaluator (AASHTO, 2013).

The procedures are categorized into some levels according to the purpose of a load rating; a design load rating, a legal load rating, and a permit load rating. A design load rating evaluates whether a bridge has adequate capacity against the strength limit state in the reliability concept of LRFD. The HL-93 design load (Table: 2.2; AASHTO, 2017) is used here.

A bridge, which does not satisfy safety at the design load rating level, is evaluated at the legal load rating level to determine a posting or a strengthening. The bridge is evaluated with AASHTO legal loads (Figure 2.3; AASHTO, 2013)

or state legal loads.

The permit level is applied to a bridge that satisfies safety against the design load or a legal load. By the needs of an owner, it evaluates safety or serviceability against a load whose weigh more than the design load or a legal load.

The load factors are defined as Table 2.16. At the legal or permit procedure, the live load factor, γ_{LL} is determined according to traffic that the rating targets to; such as traffic volume (average daily truck traffic; ADTT) and the type of load (AASHTO, 2013; Minervino et al., 2004).

The design load rating, especially, is divided into two categories; inventory and operating rating level which infers the maximum and the minimum permissible loads. Each level defines the live load factor differently.

The inventory level evaluates a bridge with the same reliability with AASHTO LRFD (AASHTO, 2017), β = 3.5, accordingly, it adopts the same γ_{LL} with the

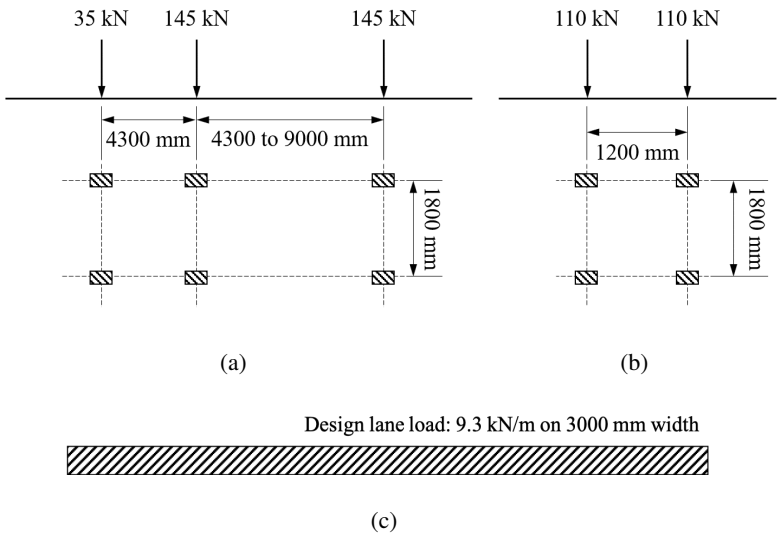

Figure 2.2: The schematic diagram of HL-93 design load specified in AASHTO LRFD Specification (2017); (a) design truck; (b) design tandem; (c) design lane load

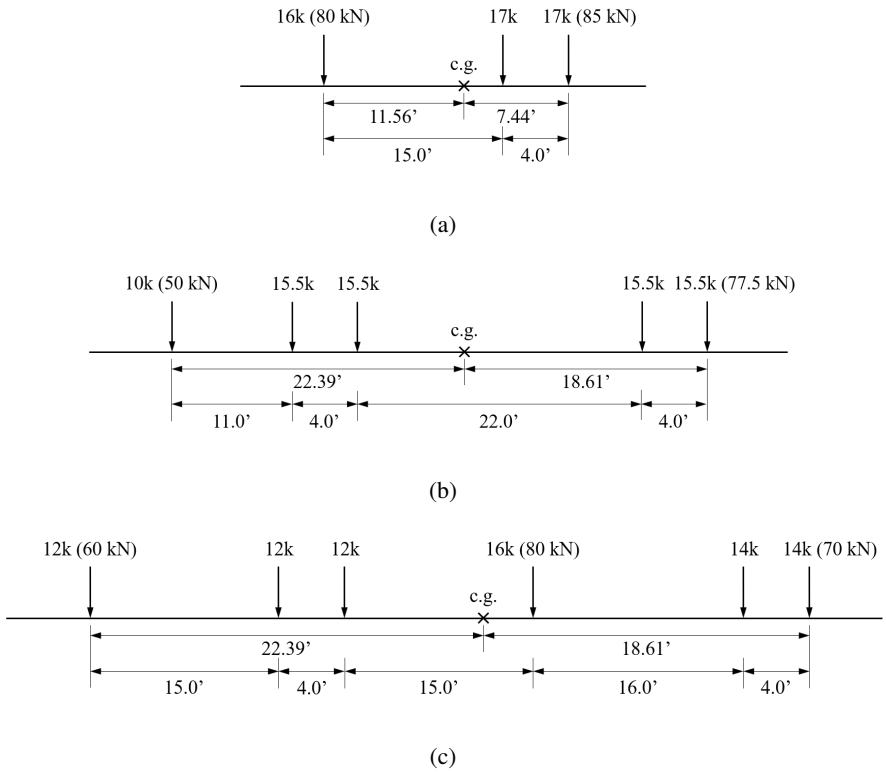

Figure 2.3: The schematic diagram of AASHTO legal truck loads; (a) Type 3; (b) Type 3S2; (c) Type 3-3. k refers to weight in kips; c.g. refers to a center of gravity

design criteria (Hwang, Nguyen, & Kim, 2013; Minervino et al., 2004; N. Wang, Ellingwood, Zureick, & O'Malley, 2009). The bridge having adequate safety about the level ($RF > 1$) is assumed to have enough capacity against the design load HL-93, moreover, all legal loads of AASHTO and State.

The operating level evaluates a bridge with the lower reliability of $\beta = 2.5$ (Hwang et al., 2013; Minervino et al., 2004; N. Wang et al., 2009). It can be said that the lower reliability reflects a lower uncertainty in an operating situation. The bridge only passes the design load screening at the operating level, will have enough capacity about AASHTO legal loads. In other words, it could not have

Table 2.16: Load factors γ_i's for a concrete bridge according to the LRFR approach of AASHTO MBE

Bridge Type	**Limit State**	**Dead Load** γ_{DC}	**Dead Load** γ_{DW}	**Design Load**		**Legal Load**	**Permit Load**
				Inventory	**Operating**		
				γ_{LL}	γ_{LL}	γ_{LL}	γ_{LL}
RC	Strength I	1.25	1.50	1.75	1.35	$*$	-
	Strength II	1.25	1.50	1.75	1.35	-	$**$
	Service I	1.00	1.00	-	-	-	1.00
PSC	Strength I	1.25	1.50	1.75	1.35	$*$	-
	Strength II	1.25	1.50	1.75	1.35	-	$**$
	Strength III	1.00	1.00	0.80	-	1.00	-
	Service I	1.00	1.00	-	-	-	1.00

$*$: refers to Table 6A.4.4.2.3a-1 and 6A.4.4.2.3b-1
$**$: refers to Table 6A.4.5.4.2a-1 of AASHTO MBE (2013)

adequate resistance upon some state legal loads which is heavier than AASHTO loads. The bridge that does not pass in this level should be evaluated with a legal load.

Minervino et al. (2004) describes that *the load factors in the manual are determined for load ratings under legal loads incorporation with the site-specific data*. Hence, the concept of the manual is independent of load models or bridge-specific data maintaining the main concept of the LRFD code.

Since the concept is the same with the current design code and adopts the lower values of live load factors based on the purpose of evaluation, the code will provide an appropriate, not conservative rating result for an existing highway bridge.

The ASD and the LFR Approach

The allowable stress rating (ASD) and the load factor rating (LFR) have been specified since the former version of AASHTO MBE, AASHTO Manual for Condition Evaluation of Bridges (AASTHO, 1994). The rating methods are defined as Eq. (2.8).

$$RF = \frac{C - A_1 D}{A_2 L(1 + I)} \tag{2.8}$$

where,

C	the capacity of a member
D	dead load effect on a member
L	live load effect on a member
I	impact factor to be used with the live load effect as specified in (AASHTO (2002))
A_1	dead load factor
A_2	live load factor

It also specifies the bridge member rating in a similar concept of the load carrying capacity defined by KISTEC (2018a, 2018b) without the factor K_s. The bridge member rating, RT is defined as Eq. (2.9).

$$RT = (RF)W \tag{2.9}$$

where,

RT	bridge member rating, tons
W	weight of nominal truck used in determining the live load effect, tons

The LFR approach defines inventory and operating level rating in a similar concept of the LRFR approach. The difference is that LFR is not the reliability concept. The concepts are defined in qualitatively such as; the inventory level is

defined as *a live load which can safely utilize an existing structure for an indefinite period of time*; the operating level is defined as *the maximum permissible live load to which the structure may be subjected* (AASHTO, 2002; AASHTO, 2013; Minervino et al., 2004). The load factors are defined as Table 2.17

Table 2.17: Load factors, A_1 and A_2 of load factor rating method of AASHTO MBE

	Allowable Stress Rating	**Load Factor Rating**	
		Inventory	**Operating**
A_1	1.0	1.30	
A_2	1.0	2.17	1.30

Table 2.18: The comparison of load factors between the load factor rating of AASHTO MBE and the strength design-based approach of Korean guideline

Load Factor	**Load Factor Rating of AASHTO MBE**	**Strength Design Based Rating of KISTEC (2018)**
Dead Load	1.30	1.30
Live Load	2.17	2.15

The impact factor, I adopted here follows the specification in AASHTO (1994), which is the same with the KISTEC (2018a, 2018b) as Eq. (2.10).

$$I = \frac{15}{(40 + L)} \leq 0.30 \tag{2.10}$$

where,

L the span length, m

Here, it can be seen that the live load factor of inventory level of LFR is similar with the one of KISTEC (2018a, 2018b). These are compared in Table 2.18.

The reason is that both are originated from the design codes which are based on ultimate strength design. Nonetheless, specifying the operating level and not adopting resistance factor, the LFR approach would lead to a less conservative result than the domestic guideline.

In both LRFR and LFR guideline, a diagnostic load test is not specified as the main task of inspection, or as a tool for detecting unknown deterioration. Besides, it is said that its important use is *to confirm the precise nature of load distribution to the main load carrying members of a bridge and to the individual components of a multi-component member* (AASHTO, 2013). It implies that the test improves the understanding of unknown behavior which is favored to the structural safety, and improves rating results.

According to AASHTO MBE, a diagnostic test may be beneficial to take advantage of bridge's extra capacity that has not been considered in the theoretical calculation; such as unintended composite action, unintended moment carrying capacity of support; participation of secondary or nonstructural components, etc. The updated load rating factor in the application of a diagnostic test is as follows;

$$RF_T = RF_c K \tag{2.11}$$

$$K = 1 + K_a K_b \tag{2.12}$$

$$K_a = \frac{\varepsilon_c}{\varepsilon_T} - 1 \tag{2.13}$$

where,

RF_T	load-rating factor for the live-load capacity based on the load test result
RF_c	rating factor based on calculations
K	adjustment factor resulting from the comparison of measured test behavior with the analytical model

K_a accounts for both the benefit derived from load test

K_b accounts for the test team's understanding and explanation of the load test results

ε_c maximum member strain measured during load test

ε_T corresponding calculated strain due to the test vehicle

2.2.2 Relevant FHWA Guidelines

For efficient bridge management, the Federal Highway Administration (FHWA) adopts a coding system. All bridges in the United States are recorded using the system, including their locations, specification, inspection results, and so on. An inspection results are reported as Figure 2.4. FHWA Recording and Coding Guide (FHWA, 1995) and its guideline, Bridge Inspector's Reference Manual (BIRM) (Thomas, Eric, Chill, & Bryan, 2012) are used to coding a bridge.

According to FHWA (1995), rating an inspection result is categorized into condition rating and appraisal rating. The material and physical condition of a deck, a superstructure, a substructure, a channel, and a culvert are evaluated for a condition rating. Its scope is not to describe localized or normally occurring instances of deterioration but to describe the general condition of entire components. The rating is coded in 10 levels as Table 2.19.

Appraisal rating determines whether a bridge can provide the level of service as a part of a highway system. It is coded as Table 2.20, for structural evaluation, deck geometry, underclearances, waterway adequacy, and approach roadway alignment. The lowest of a superstructure condition rating, a substructure condition rating, and an inventory level load rating is determined as the structural evaluation rating (Table 2.21).

The guideline suggests that the bridge posting is performed for a bridge not pass the operating level and coded comparing the rating result to maximum legal

PDT Form D-450K (DEC 1996) **Bridge 2 Data** Inspection Date

A01 | 0 2 | 7 4 2 1 | 0 0 0 0 | 9 0 6 1 | E06 | 0 6 2 3 1 1

E19 Paint Condition | 8 8 | New Paint Y / N | If Yes: [ ] Spot [ ] Zone [X] Full [ ] Revise item G08-G17

Interior Beam / Girder: VERY GOOD - RECENTLY REPAINTED.

Fascias: VERY GOOD - NEW.

Splash Zone: Truss / Girder:

Truss:

Bearings: VERY GOOD.

Other:

E23 Est. Remaining Life | BMS to Calculate Yes/No | 3 4 | Comments:

Recalculate IR/OR: Yes [ ] Due to: Deterioration [ ] New Wearing Surf. [ ] Other [ ]

No [X] Previous Rating Dated _____ is still valid

E30 Inventory Rating	1 9 8	2 9 8	8 9 8			2 9 8
E31 Operating Rating	1 9 8	2 9 8	8 9 8			2 9 8
	H	HS	ML-80	Other	Other	HS Load Factor

E32 Rate Meth | 2 S | E33 Typ Mem | 1 | AASHTO | E37 Spec | 9 4 | E38 Manual | 9 4

E29 Bridge Post | 9 | CONTROLLING: H ____ HS ____ ML80 X Engineering Judgement ____

E24 Structural Condition Appraisal | 7 | Based upon [ ] Table 1 B27-ADT ____ B30-IR ____

or E18-Super 7 E20-Sub 7 , E22-Culvert ____ ,

E01 Next Insp. Freq. | 2 4 | E03 Equip. Next Insp. | B | SNOOPER TRUCK (UB-40)

E04 Spec. Insp. Type | | E05 By Date | |

Is bridge over water? [X] Yes. E22 = N Complete Forms D-450E through G

[ ] No. E22 = N E21 = N E27 = N E29A = N

Notes: ONE SPAN IS OVER WATER AND ONE SPAN IS OVER RAILROAD.
HAD RAILROAD REPRESENTITIVE ON SITE. CREW WAS OUT OF SPAN 1 (RR LOCATION) BY TIME
REQUIRED. (9 A.M.)
INSPECTION WAS FIRST ON NEWLY CONSTRUCTED BUSWAY BRIDGE.WHICH USED AN EXISTING RR BRIDGE.
CONDUITS ON BRIDGE WERE BUSTED AT ADAPTERS AT ABUTMENT 1. ALSO, ONE EXPANSION COUPLER WAS
BROKEN AND NEEDED REPLACED. SEVERAL CONDUIT SEGMENTS IN SPAN 1 WERE SEVERELY BUCKLED
AND NEEDED REPLACED.

Signatures and Date: PATRICK LEACH, P.E. - 6/23/11
CHARLES MOLNAR - 6/23/11

Figure 2.4: The example of reporting an inspection result of a United States highway according to Recording and Coding Guide

Table 2.19: Component condition rating according to Federal Highway Administration (FHWA) (1995)

Code	Description
N	NOT APPLICABLE
9	EXCELLENT CONDITION
8	VERY GOOD CONDITION - no problems noted.
7	GOOD CONDITION - some minor problems.
6	SATISFACTORY CONDITION - structural elements show some minor deterioration.
5	FAIR CONDITION - all primary structural elements are sound but may have minor section loss, cracking, spalling, or scour.
4	POOR CONDITION - advanced section loss, deterioration, spalling, or scour.
3	SERIOUS CONDITION - loss of section, deterioration, spalling or scour have seriously affected primary structural components. Local failures are possible. Fatigue cracks in steel or shear cracks in concrete may be present.
2	CRITICAL CONDITION - advanced deterioration of primary structural elements. Fatigue cracks in steel or shear cracks in concrete may be present or scour may have removed substructure support. Unless closely monitored it may be necessary to close the bridge until corrective action is taken.
1	”IMMINENT” FAILURE CONDITION - major deterioration or section loss present in critical structural components, or obvious vertical or horizontal movement affecting structure stability. Bridge is closed to traffic but corrective action may put bridge back in light service.
0	FAILED CONDITION - out of service; beyond corrective action.

load.

Though the appraisal rating is determined as the domestic guideline, FHWA (1995) has a detailed rating system. And it specifies that every item of inspection does not need to be performed. Moreover, it evaluates a bridge as a part of a road system. In other words, it is not rated as an independent structure. Also, the criteria for the coding condition of a structure is not specified quantitatively. Hence, the assessment will be more efficient and complex procedure leaving a room for engineer’s decisions.

Table 2.20: Appraisal rating according to Federal Highway Administration (FHWA) (1995)

Code	Description
N	Not applicable
9	Superior to present desirable criteria
8	Equal to present desirable criteria
7	Better than present minimum criteria
6	Equal to present minimum criteria
5	Somewhat better than minimum adequacy to tolerate being left in place as is
4	Meets minimum tolerable limits to be left in place as is
3	Basically intolerable requiring high priority of corrective action
2	Basically intolerable requiring high priority of replacement
1	This value of rating code not used
0	Bridge closed

Table 2.21: Inventory level rating code according to Federal Highway Administration (FHWA) (1995)

Rating Code	**Inventory Rating**		
	Average Daily Traffic (ADT)		
	0-500	**501-5000**	**> 5000**
9	> 32.4 (MS18)	> 32.4 (MS18)	> 32.4 (MS18)
8	32.4 (MS18)	32.4 (MS18)	32.4 (MS18)
7	27.9 (MS15.5)	27.9 (MS15.5)	27.9 (MS15.5)
6	20.7 (MS11.5)	22.5 (MS12.5)	24.3 (MS13.5)
5	16.2 (MS9)	18 (MS10)	19.8 (MS11)
4	10.8 (MS6)	12.6 (MS7)	16.2 (MS8)
3	Less than rating code of 4 and requiring corrective action		
2	Less than rating code of 4 and requiring replacement		
0	Bridge closed due to structural condition		

2.3 ACI 562-16: Code Requirements for Assessment, Repair, and Rehabilitation of Existing Concrete Structures (2016, US)

ACI 562-16 (ACI 562 Committee, 2016) can be used to assess and determine repair or rehabilitation of existing building and non-building concrete structures. According to this, an existing structure is categorized as; unsafe structural condition (Eq. (2.14)); substantial structural damage; conditions of deterioration, faulty construction or damage less than substantial structural damage (Eq. (2.15)). Its evaluation criterion is represented by the reciprocal of safety factor as Eqs. (2.14), (2.15).

A structure satisfies Eq. (2.14) is in a condition whose safety cannot be insured against collapse. The factor ϕ can be used as the same value of ACI 318 (ACI 318 Committee, 2014). Its value can be raised to the value specified in ACI 562; for instance, resistance factor for a tension-controlled member can be raised to 1.0

$$\frac{U_c}{\phi R_{cn}} > 1.5 \tag{2.14}$$

$$\frac{U_o}{\phi_o R_{cn}} > 1.0 \tag{2.15}$$

where,

R_{cn} current in-place nominal capacity including the effects of damage, deterioration

U_c demand using nominal loads of the current building code and factored load combinations of ASCE/SEI 7

U_o demand using nominal loads and factored load combinations of the original building code

ϕ_o resistance factor of the original building code

Among the structure in unsafe structural condition, one who satisfies Eq. (2.15) needs repair or rehabilitation. The reason why the safety of a structure is evaluated additionally in Eq. (2.15) is that the structure might be evaluated to have enough capacity when the original building code is applied.

It specifies that strength losses of materials, section losses of reinforcements, alkali-silica reaction or delayed ettringite formation could be considered in R_{cn}, however, it is conceptual.

2.4 BD 21/01: The Assessment of Highway Bridges and Structures (2001, UK)

BD 21/01 (The Highways Agency, 2001) is one part of United Kingdom's design manual for roads and bridges. It adopts partial safety factor of Eurocode to assess a structural safety. It evaluates a structure with a simple relation between the capacity and the demand of a structure, as Eq. (2.16).

$$R_A^* \geq S_A^* \tag{2.16}$$

where, R_A^* refers to an assessment resistance, and S_A^* refers to an assessment load effect. These are defined as Eqs. (2.17) and (2.18), respectively.

$$R_A^* = F_c \cdot R^* \tag{2.17}$$

$$S_A^* = \gamma_{f3}(\text{effects of } Q_A^*) \tag{2.18}$$

where,

F_c condition factor

R^* the resistance of a structure; which is funtion of f_k/γ_m

Q_A^* assessment load; which is $\gamma_{fL}Q_k$

f_k the specified strength of a material

Q_k nominal load

γ_{f3} the factor reflecting the inaccuracy of an analysis model or an load effect such as stress distribution

= 1.1 for usual assessment

= 1.0 if such inaccuracy is verified through a test

γ_{fL} load factor for each Q_k

= 1.15 for dead load by concrete

= 1.75 for surfacing material

= 1.50 for live load

γ_m the partial factor for a material as specified in the Eurocode

= 1.50 for concrete

= 1.15 for reinforcing steels or prestressed tendons

The f_k of concrete can be determined by a test according to a guideline BD 44/15 (The Highways Agency, 2015). Also, The Highways Agency (2001) suggests that the f_k of a corroded reinforcement should be determined by a test when its section loss is more than 50%. Otherwise, the specified design strength of the reinforcement is used as the value f_k.

2.5 Reliability-Based Safety Assessment Guidelines of Expressway Bridges (2013, Korea)

In South Korea, KECRI (2013a, 2013b) developed reliability-based load rating guideline. However, this guideline is not regulated in law, and not used practi-

cally. The criteria are similar to the load rating of AASHTO MBE or BD 21/01. The relationship Eq. (2.19) is proposed in the guideline.

$$R_A \geq U_A \tag{2.19}$$

where, R_A and U_A refer to the assessment resistance and the load effect, respectively, and they are defined as Eqs. (2.20) and (2.21).

$$R_A = \phi_A R_i \tag{2.20}$$

$$U_A = \sum \gamma_A U_i \tag{2.21}$$

where,

R_i	resistance; function of $\phi_j X_j$
U_i	load effect; $(= \gamma_i Q_i)$
γ_A	load assessment factor
ϕ_A	resistance assessment factor
Q_i	nominal load specified in KHBDC (MOLIT, 2016b)
X_j	the specified strength of a material
γ_i	load factor for a safety assessment
ϕ_j	material resistance factor as specified in KHBDC (MOLIT, 2016b)

The determination of resistance is based on material resistance factor which is the same as the current design code (MOLIT, 2016b), as a result, the concept of assessment is identical to the current design concept.

Here, the ϕ_A is proposed, and it is the same concept of the condition factor in AASHTO MBE. Also, its value is proposed as Table 2.22. The factor γ_A reflects the discrepancy between design load model and the actual load in operation, and it is suggested as Table 2.23. The load factors are specified as Table 2.24.

The concept of load factor is similar to the LRFR of AASHTO MBE. It divides the assessment live load level into two categories; a design live load

Table 2.22: Resistance assessment factor, ϕ_A according to the Reliability-Based Safety Assessment Guideline of Expressway Bridges

Condition Rating of a Member	**Resistance Assessment Factor, ϕ_A**
A, B	1.00
C	0.95
D, E	0.85

Table 2.23: Load assessment factors, γ_A according to the Reliability-Based Safety Assessment Guideline of Expressway Bridges

Dead Load, γ_{AD}		**Live Load, γ_{AL}**	
Design	**Measured**	**Design**	**Permissible**
1.00	0.90	0.90	1.00

Table 2.24: Load factors, γ_i according to the Reliability-Based Safety Assessment Guideline of Expressway Bridges

Dead Load, γ_D		**Live Load, γ_L**	
γ_{DC}	γ_{DW}	**Design**	**Permissible**
1.25	1.50	1.80	1.30

and a permissible live load. Here, the design load that the guideline targets to is KL-510 load (Figure 2.5) specified in the current design code of South Korea (MOLIT, 2016b). The guideline set a reliability index of β = 3.5 on design load assessment which is the same with the design code, and β = 2.5 on permissible load assessment Hwang et al. (2013). In other words, each has the same concept with the inventory or the operating rating level of AASHTO LRFR method.

The difference is the load assessment factor γ_A. For design load rating, the live load factor is reduced to reflect the decreased uncertainty between the design and the operating situation where the location and traffic characteristics

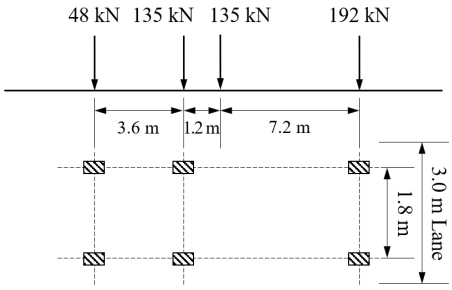

(a) Design truck load

Design land load, $w = \begin{cases} 12.7 & \text{kN/m, for } L \geq 60 \text{ m} \\ 12.7 \times (60/L)^{0.10} & \text{kN/m, for } L \geq 60 \text{ m} \end{cases}$ on 3 m width

(b) Design lane load

Figure 2.5: The schematic diagram of KL-510 design load specified in Korean Highway Bridge Design Code (Limit State Design) (2016)

affect (KECRI, 2013a; 2013b)).

According to the guideline, the safety rating is determined by the safety factor and the rating factor as defined in Eqs. (2.22) and (2.23). The criterion is the same with that of the current guideline as Table 2.13.

$$SF = \frac{R_A}{U_A} \tag{2.22}$$

$$RF = \frac{\phi_A R_i - \gamma_{AD}\gamma_D D}{\gamma_{AL}\gamma_L L(I)} \tag{2.23}$$

where,

D	dead load effect
$L(I)$	live load effect considering impact factor of 0.25; for all limit state except for fatigue limit state (MOLIT, 2016b)

2.6 Summary

Every guideline specifies on-site investigation, material test, and load rating. The details were slightly different from each other. Load rating method showed the biggest difference. Some evaluate structural safety with a safety factor, while others, as a rating factor. Especially, the domestic guidelines adopt both factors to evaluate safety. Also, each guideline specifies the concept and the value of load and resistance factor differently as in Table 2.25. Consequently, the differences will provide diverging results of SF, RF and also the safety rating for one same bridge.

As discussed above, the concept of the current domestic guideline (KISTEC, 2018a; 2018b) is identical to the former design code. Accordingly, large live load factor will yield a conservative result as the former design code had yielded, in other words, it will have the discrepancy with the current code.

The reliability-based guideline of Korea (KECRI, 2013b), whose concept is identical to the current design code, will be the best solution to resolve the discrepancy. The low value of load factor considering the operating situation will yield appropriate results for existing concrete bridges maintaining the current design concept.

In Korea and the United States, structures are rated in code; from A to E or from 9 to 0, according to inspection results. Especially, only in Korea, every specified item is rated individually, also, the rating criteria are so deterministic that any engineer's decision cannot intervene in the assessment procedure. Moreover, inspections even on sound elements have to be conducted at any cost. As a result, the assessment will be an expensive and inefficient procedure.

Unlike the Korean guideline, AASHTO MBE specifies that the change from initial or pre-recorded condition should be monitored without clarifying which item must be inspected. Also the interval of in-depth inspection is not specified

clearly; it can be conducted after an initial or a damage inspection.

Hence, to save an effort to assessment, the revision of the domestic guideline should be toward to the concept of the U.S. which leaves a room for engineer's decisions. As parts of verifying the discussions, load rating method and material test evaluation criteria have been examined in the following chapter.

Table 2.25: Comparison of load rating methods specified in each guideline

	KISTEC (2018)	**AASHTO MBE (2013)**	**ACI 562-16 (2016)**	**BD21/01 (2001)**	**KECRI (2013)**
SF	$\frac{\varphi M_n}{M_u}$ or $\frac{f_a}{f_{d+l}}$	-	$\frac{U_c}{\phi R_{cn}}$ or $\frac{U_o}{\phi_o R_{cn}}$	$R_A^* \geq S_A^*$	$\frac{R_A}{U_A}$
RF	$\frac{\varphi M_n - \gamma_d M_d}{\gamma_l M_l(1+i)}$ or $\frac{f_a - f_d}{f_l(1+i)}$	$\frac{C-(\gamma_{DC})(DC)-(\gamma_{DW})(DW)\pm(\gamma_P)(P)}{(\gamma_{LL})(LL+IM)}$ or $\frac{C-A_1 D}{A_2 L(1+I)}$	-	-	$\frac{\phi_A R_i - \gamma_{AD}\gamma_D D}{\gamma_{AL}\gamma_L L(I)}$
Load Factor	$1.3D + 2.15L$	LRFR $1.25DC + 1.75(LL+IM)$ $1.25DC + 1.35(LL+IM)$ LFR $1.30D + 2.17L(1+I)$ $1.30D + 1.30L(1+I)$	$1.2D + 1.6L$	$1.27DC + 1.65L$	Design $1.25DC + 1.63L(I)$ Permis-sible $1.25DC + 1.30L(I)$
Resist-ance Factor*	0.85**	LRFR Condition/System Factor 0.85 ~ 1.00 LFR Not applied	0.90 ~ 1.00	partial factor for material**	material resistance factor**

*: the resistance factor of a prestressed member

**: refers that the value is the same as defined in a current national design code

Chapter 3 Verification of Performance Assessment by Case Studies

For the validity analysis, actual assessments on concrete bridges were needed to be examined. The study targeted concrete highway bridges and flyovers in Seoul; not on the Han River. Most of them are designated by Class II establishment, and have been undergone full safety inspections for every two years. Hence they are concerned to be in blind-spot of maintenance while they have been under heavy traffic demands.

First, assessment reports were collected which has been opened to the public on the Internet through Opengov system of the Seoul Metropolitan Government. Among 230 bridges managed by the the Seoul Government, the targets were reduced to 29 bridges' cases. They had been constructed between 1966 and 1987, most of them are prestressed concrete bridges. The total length is 7,371 m.

Reports of the bridges were collected through the Seoul Metropolitan Government and affiliated offices. However, there were some documents that had been lost and cannot be found. Hence, the scope was narrowed to 14 concrete bridges whose design drawings and relevant documents sufficiently exist.

To validate the structural safety rating, load ratings were conducted adopting the approaches in chapter 2. Also, diagnostic load tests were conducted on one of the cases, then, the results were examined to validate the domestic guideline. Among the conditional safety rating items, the material tests were validated by analyzing test records in the reports.

Table 3.1: Examined concrete bridge cases in the validity analyses

Case id.	Type*	Built Yr.	Conditional Safety	Structural Safety	Span, m	Strength, kN-m**	Design Loads
1	PSC I	1966	**B**	A	22.6	7,765	DB-18/ DL-18
2	PSC I	1966	**B**	A	18.0	6,851	DB-18/ DL-18
3	RC T	1966	**B**	A	11.8	4,328	DB-18/ DL-18
4	PSC I	1968	**C**	B	29.9	8,318	DB-24/ DL-24
5	PSC I	1968	**C**	A	28.9	6,119	DB-18/ DL-18
6	RC S	1968	**C**	A	11.0	760	DB-18/ DL-18
7	PSC I	1970	**B**	A	20.0	10,047	DB-24/ DL-24
8	PSC I	1976	**B**	A	28.4	12,365	DB-18/ DL-18
9	PSC I	1977	**C**	A	29.8	13,327	DB-18/ DL-18
10	PSC I	1977	**C**	A	24.9	8,841	DB-18/ DL-18
11	PSC I	1979	**B**	A	25.5	8,312	DB-18/ DL-18
12	PSC I	1983	**B**	A	20.0	7,978	DB-24/ DL-24
13	PSC I	1984	**C**	A	30.5	13,558	DB-24/ DL-24
14	PSC I	1986	**C**	B	14.9	3,510	DB-24/ DL-24

$*$: PSC I - prestressed concrete I beam; RC T - reinforced concrete T beam;
RC S - reinforced concrete slab.
$**$: representative values; derived by sectional analyses.

3.1 Verification of Load Ratings

3.1.1 Load Rating Methods

To validate the structural safety evaluating method of Korea, load ratings about 14 cases, applying all methods investigated in the previous chapter, were conducted. The cases are summarized in Table 3.1. For all cases, conditional safety ratings governed the safety ratings of bridges.

For a few cases, there were missed drawings and information such as reinforcing steel placement or jacking forces of tendons, proper assumptions were made referring to the drawings of similar bridges.

Resistance Calculation Procedures

In calculating the capacity of each bridge section, to reflect the conventional approaches, the study followed the approach of a design code that every guideline is based on. Such as MLTM (2010) for the current domestic guideline; AASHTO (2017) for LRFR method of AASHTO MBE; AASHTO (2002) for LFR method of AASHTO; ACI 318 Committee (2014) for ACI 562-16; CEN (2005) for BD 21/01; MOLIT (2016b) for the reliability-based method of KECRI. Every effective width provision is examined, however, it was fixed to the provision of MOLIT (2016b) to focus on the differences in load rating provisions. Also, the sections are limited to interior girders, see the gray section of Figure 3.1.

For PSC I members, especially, strain compatibility analyses were made to predict strains of tendons in the ultimate limit state. In consideration of stress losses of tendons, proper assumptions were made.

Sections were set as the design drawings; since the sectional losses are not recorded in the reports it is not available to introduce actual dimensions to load

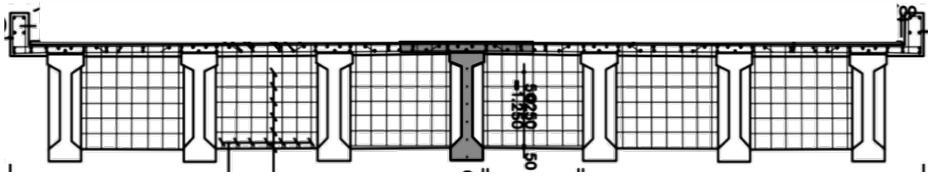

Figure 3.1: Example of target section for load rating verification

ratings. To verify computed resistances, results were compared to the moment resistances calculated by sectional analyses. The procedures were made with the author's program coded in MATLAB. Detailed calculation procedures are covered in Appendix A for some representative cases.

Load Effect Calculation

The dead load effects were calculated considering haunches and lateral beams. Wearing surfaces' effects are assumed to be negligible. For a live load effect, the design load of each bridge was considered first, to compare the distinctions in load rating provisions.

This approach might result in inconsistencies of reliability, however, the commentary of AASHTO MBE suggests that legal load can be used with slight bias (AASHTO, 2013). Moreover, since the design loads in LRFD codes are notional, they are hard to be applied in a posting (AASHTO, 2013). Thus, the study has decided that load ratings based on the design loads in Table 3.1 can provide reasonable results.

Additionally, loads that each guideline supposed for load rating are considered, to see if the load ratings will result in the similar result when the target load that corresponds to the concept of each guideline; that is, HL-93 to LRFR of AASHTO MBE and KL-510 to the KECRI guideline.

Live load effects were computed with the author's program coded by MATLAB. It adopted live load moment distribution factor specified in AASHTO

LRFD. To verify the results, they were compared with frame analyses results by a commercial program (MIDAS Civil), which are given in the assessment reports. As a result of the comparison, the code was verified to result in reasonably accurate answers with the differences around 0.5%.

Load Rating Results

Figure 3.2 presents the load rating results based on the actual design loads. The results by the domestic guideline are indicated in KISTEC, which is the solid circle. ACI 562 results are expressed in two ways; min. and max. refer to the minimum and the maximum of a resistance factor. Both inventory and operating level rating results of LRFR and LFR of AASHTO MBE are presented. Likewise, both the design load and permissible rating method of KECRI are presented. The condition factors of LRFR and BD 21/01 are determined using the KECRI's provision.

As seen in Figure 3.2 all results were above 1.0, however, values of SF and RF were dispersed. That is, every guideline has evaluated one structure with different safety level. To be specific, for SF, the ratio of the maximum to the minimum varied from 1.48 to 1.75; for RF, from 2.00 to 2.20. Also, according to the observation of results, the study found that the Korean guideline (KISTEC) evaluates bridge's safety or live load margin most conservatively.

Load ratings based on the design loads specified in guidelines (Figure 3.3) resulted in slight changes in trends. DB and DL loads were used in KISTEC, LFR and permissible rating of KECRI; HL-93 design load was used in LRFR; KL-510 load was used in design rating of KECRI. To see the effect of live load on a safety factor, only KISTEC and KECRI results are shown in Figure 3.3(a).

The results were different from the previous results in a number of respects. The former SF were diverged with the ratio maximum/minimum from 1.20 to

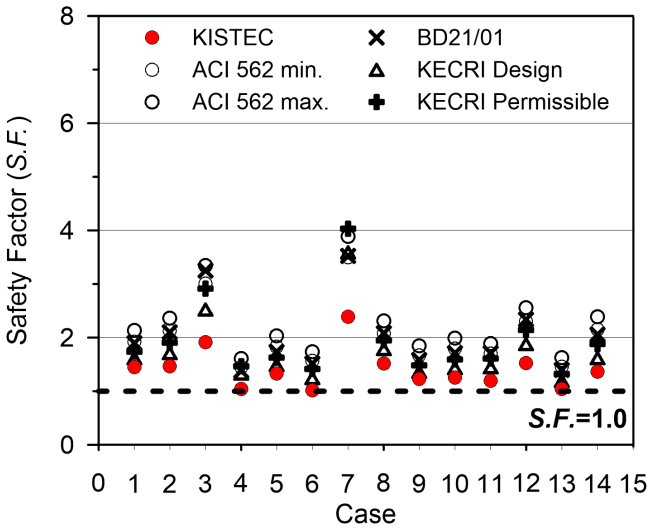

(a)

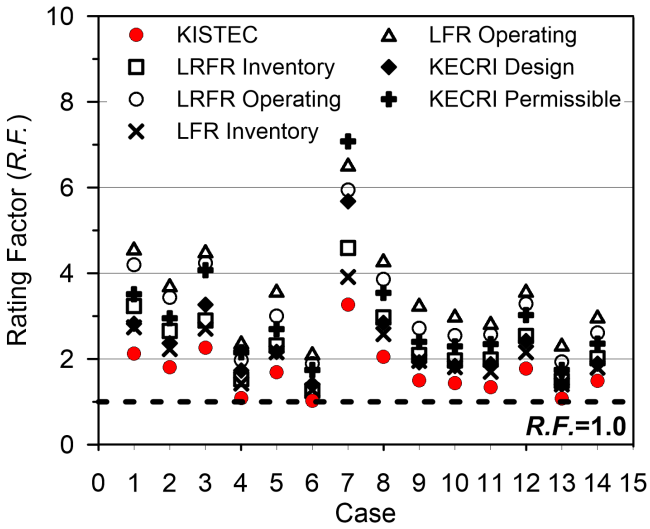

(b)

Figure 3.2: Load ratings according to provisions of guidelines with DB and DL design load

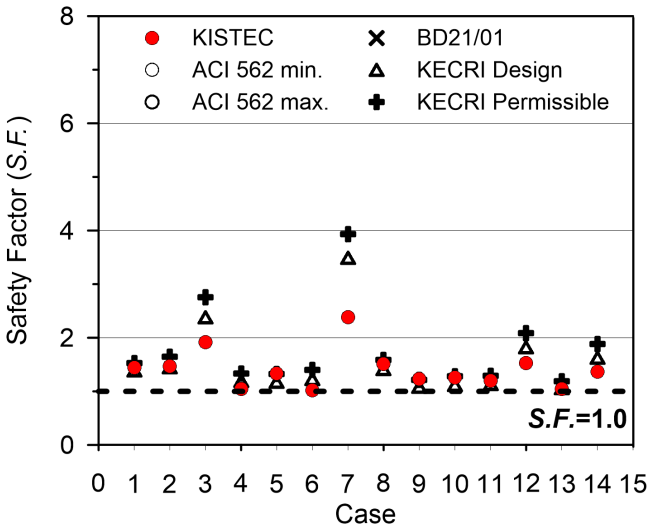

(a)

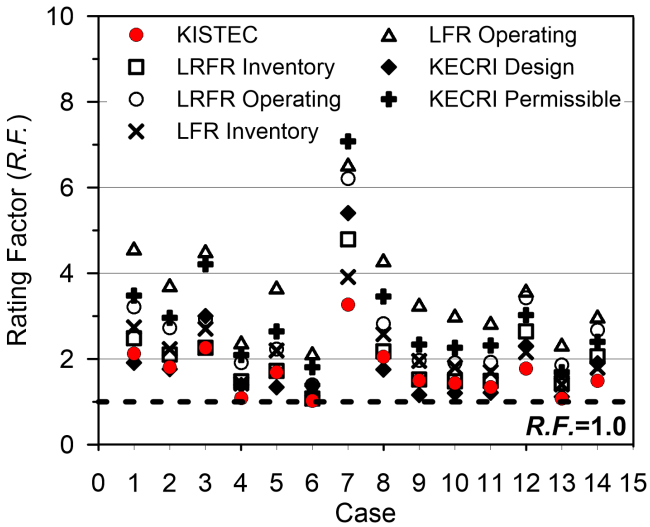

(b)

Figure 3.3: Load ratings according to provisions and the design loads specified in guidelines

1.69 among KISTEC and KECRI. By contrast, The results in Figure 3.3 diverged with the ratio from 1.10 to 1.58. The dispersion was slightly reduced. Moreover, the KISTEC result was not the minimum for every case, because the load effects from KL-510 or HL-93 load were larger than that from DB/DL loads. The cases that KISTEC still showed the minimum values were the cases built in DB-24/DL-24 loading since the effects of DB-24/DL-24 were similar to those of KL-510 or HL-93.

For RF in Figure 3.3(b), KECRI design, AASHTO LRFR inventory level, KISTEC showed similar values. Hence, adopting the reliability-based load rating approach for DB-24/DL-24 concrete bridges will not cause an argument. Nonetheless, the applicability for DB-18/DL-18 bridges needs to be examined.

Also, it has been observed that the operating level of AASHTO and permissible load ratings of KECRI have guaranteed safety of from 2 to 7 times to the design load. Hence, by verifying their validity closely, through experimental and analytical approaches, they are expected to be adopted in the domestic guideline for economic maintenance.

3.1.2 Diagnostic Load Test and Load Carrying Capacity

Static diagnostic load tests were made on the case 8 bridges in two times as a part of experimental verification. Tested span, load cases were as shown in Figure 3.4.

Finite element analyses were made using the commercial program, DIANA FEA. According to the design drawing and measured location of tested trucks, finite element model was constructed with 3D solid elements. Linear elastic behavior was assumed. Accordingly, reinforcing steels were not modeled and material property of concrete is modeled as a linear model as Table 3.2.

Here, girders are designated as G1 to G7, from left to right in Figure 3.4(b).

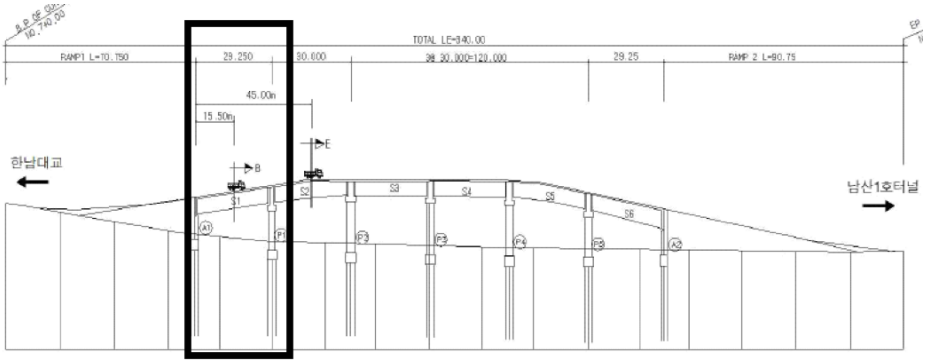

(a) Tested span; in the middle of the first span

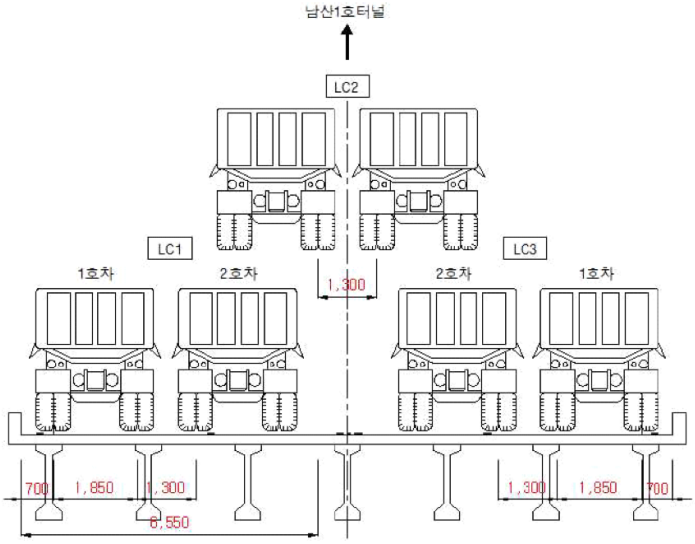

(b) Tested load cases

Figure 3.4: Span and load cases of the diagnostic load test on the case 8

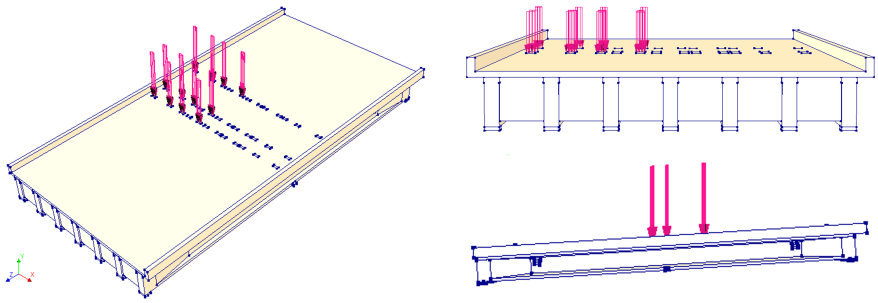

(a) Geometrical modeling

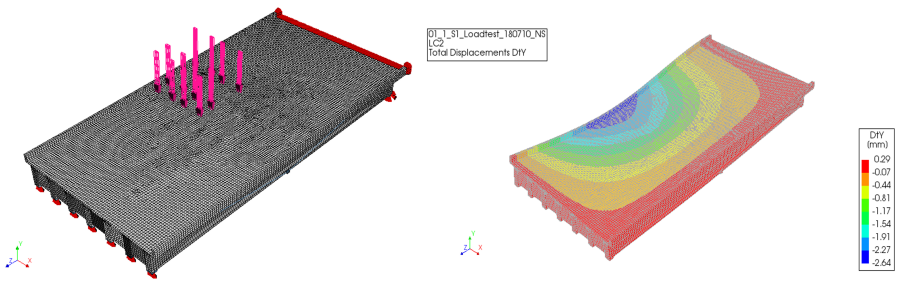

(b) Discretized model and its analysis result

Figure 3.5: Finite element analysis of the diagnostic load test using DIANA FEA

Table 3.2: Material properties of concrete used in the finite element analyses

	Component	**Value**
Compressive Strength	Girder	f_{ck} = 50.0 MPa (Rebound hammer test 16')
	Deck	f_{ck} = 26.7 MPa (Rebound hammer test 16')
Elastic Modulus	Girder	E_c = $31,314$ MPa
	Deck	E_c = $25,405$ MPa
Poisson's Ratio	Common	ν = 0.18
Density	Common	ρ = $2,350$ kg/m^3

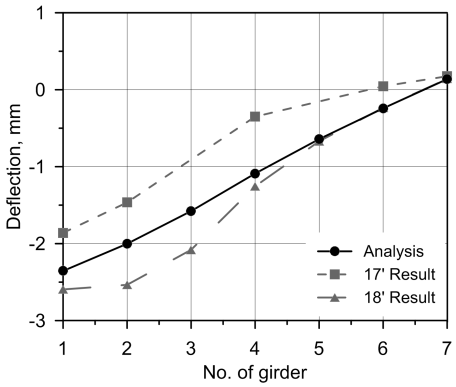

(a) Load case 1

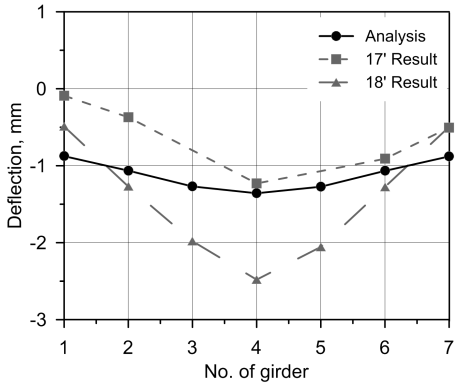

(b) Load case 2

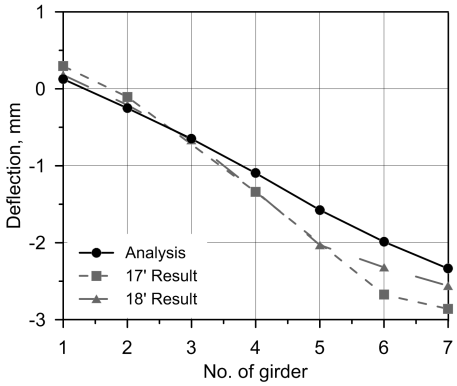

(c) Load case 3

Figure 3.6: Comparison of displacements between the tests and the analyses

Static displacements were measured at the centers of girders; at girder 1, 2, 4, 6, and 7 in the first test; at every girder in the second test. The tests were conducted according to (KISTEC (2018a, 2018b)). For one load case, the trucks were loaded twice in every test. Figure 3.6 shows the tests and the analyses results. The 17' result refers to the first test and the 18' result refers to the second. Table 3.3 presents the tests and analyses results. Here, girder 3 and 5 are omitted since the responses of the girders are not measured in the first test.

Inconsistent trends have been observed between the first and second tests.

Table 3.3: Comparison of displacements between the diagnostic tests and the analyses; and response ratios

Load Case	Girder ID	1st Test			2nd Test		
		Test, mm (1)	Analysis, mm (2)	(2)/(1)	Test, mm (4)	Analysis, mm (3)	(4)/(3)
LC1 (Left)	G1	-1.86	-2.45	1.32	-2.59	-2.35	**0.91**
	G2	-1.47	-2.08	1.42	-2.52	-2.00	**0.79**
LC2 (Mid)	G4	-1.23	-1.42	1.16	-2.47	-1.36	**0.55**
LC3 (Right)	G6	-2.68	-2.04	**0.76**	-2.32	-1.99	**0.86**
	G7	-2.86	-2.36	**0.83**	-2.51	-2.34	**0.91**

Responses of the first test were not symmetrically distributed laterally, while those of the second test was not. The ratio of analysis to test in Table 3.3 below zero implies a stiffness degradation. The ratio in the first test was below zero for only G6 and G7. However, at the second test, It was below zero for all girders. In other words, the stiffness losses of G6 and G7 can be assumed by the first test, while the overall stiffness loss can be assumed by the second test.

For the load case 2, the large difference in displacement at girder 4 was observed. The second test result was similar to the response of a structure without lateral beams, in other words, their load redistribution capacities might be degraded. The first test result was similar to the prediction made in the thesis. It is not sure that which results deducted accurate responses.

Table 3.4 presents the values of K_s computed according to the tests and analyses results, and the load carrying capacity in terms of a RF, denoted by updated RF, which is $K_s \times RF$. As can be seen in the table, all girders' load carrying capacities (updated RF) were calculated to be over 1.0. However, the major finding was that because of the difference between the first and the second test, the stiffness change and the load carrying capacity of a section could not

Table 3.4: Comparison of calculated response compensating factors and load carrying capacity (updated RF)

Location	K_s		Updated RF	
	1st Test	**2nd Test**	**1st Test**	**2nd Test**
G1	1.44	**0.99**	2.93	2.04
G2	1.54	**0.87**	3.15	1.79
G4	1.29	**0.67**	2.63	1.38
G6	**0.93**	**0.92**	1.90	1.89
G7	1.01	1.02	2.06	2.10

be determined consistently. These results are not appropriate to be used in determining repair or maintenance. Hence the test does not have to be performed in an assessment if these random errors occur repeatedly.

3.2 Verification of Material Tests

In a full safety inspection of Korea, a rebound hammer test and a carbonation depth measurement are obligatorily conducted in every 2 years. The guideline specifies that the rebound hammer test is conducted in every 50 m for a superstructure, and the carbonation depth is measured in between 2 and 6 points (KISTEC, 2018b). However, in some cases tests records were not traceable, as in Table 3.5. In the section, with traceable sets of test data, trends of durability changes were examined. From the trends, the problems in evaluating methods were investigated.

3.2.1 Rebound Hammer Test

In the guideline (KISTEC, 2018b), rebound hammer test is specified to be used in comparative evaluation between sound and unsound points. However, in a

Table 3.5: Example of material test records for the case 5 bridge

Case ID	Built Yr.	Safety Rating	Assessed Yr.	Rebound Hammer	Carbonation Depth
1	1966	B	2006	On some spans (deck&girder)	On some spans (deck)
			2008	On some spans (deck&girder)	Not conducted
			2010	On substructure only	Not conducted
			2012	On some spans (deck&girder)	On some spans (deck)
			2014	On some spans (deck&girder)	On some spans (deck)
			2016	On some spans (deck&girder)	On some spans (deck)

practical inspection, an estimated strength from the test and design strength have been compared.

To estimate the compressive strength of concrete, the following equations are usually used (KISTEC, 2018b); Eqs. (3.1) and (3.2) are used for low strength concrete, such as a deck concrete; (3.3) and (3.4) are used for high strength concrete, such as a girder concrete.

$$f_c = -18.0 + 1.27R_0 \tag{3.1}$$

$$f_c = (7.3R_0 + 100) \times 0.098 \tag{3.2}$$

$$f_c = 1.72R_0 - 21.4 \tag{3.3}$$

$$f_c = (15.2R_0 - 112.8) \times 0.098 \tag{3.4}$$

where,

f_c estimated compressive strength of concrete, MPa

R_0 calibrated rebound value

These are empirical formula. In the precedent researches, (Chungnam National University, 2002; Ju, Park, & Oh, 2017; Kwon, Park, & Kim, 2006; Seoul National University, 1998) showed that each equation results varying presumed strength. For instance, with the same rebound value, the strength estimated by Eq. (3.3) or (3.4) is 10~20 MPa larger than one by Eq. (3.1) or (3.2).

Hence, the way of estimating a strength is not clear that it denotes the actual one. Moreover, in the collected reports, there has been a discrepancy in a design strength, having been changed even in the same bridge's reports. It seems that a specified strength is also estimated by an inspector when it is not elucidated in a design drawing. The assumption seems to be made according to the trend of a rebound hammer test.

Also, the estimated value was not used in a load rating. For instance, though the strength was estimated in 50 MPa for a structure whose design strength of 40 MPa, the inspector used the design strength for a conservative assessment.

To account for these issues, the thesis analyzed the trends of the test, performed on the five cases of bridges. The raw data of tests were analyzed in here.

Here, for reasonable estimations of strengths, additional equations validated through the preceded researches (Ju et al., 2017; Seoul National University, 1998) were considered. In addition to the above equations, Eq. (3.5) and (3.6) are used to predict the strength of a deck concrete, and Eq.(3.7) is used for a girder concrete.

$$f_c = (-120.6 + 8.0R_0 + 0.0932R_0^2) \times 0.098 \tag{3.5}$$

$$f_c = (14.6R_0 - 233.0) \times 0.098 \tag{3.6}$$

$$f_c = 1.267R_0 + 0.7868 \tag{3.7}$$

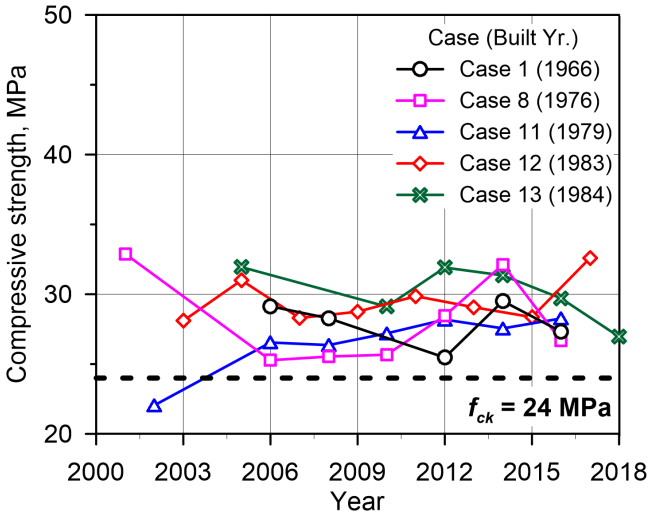

(a) Deck concrete

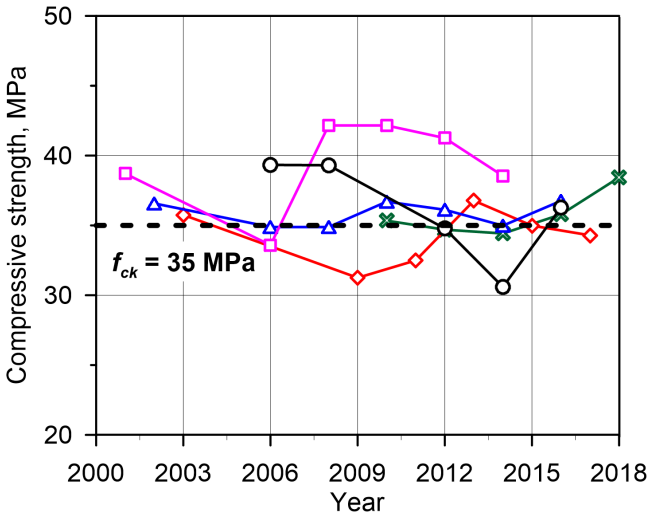

(b) Girder concrete

Figure 3.7: Records of estimated compressive strengths from the data in collected inspection reports; each dashed line refers to the representative specified strength

The analyzed results are shown in Figure 3.7. There was no tendency in compressive strength. The bias of the test comes from the changes in test spots. For one bridge, the tests had not been performed in the same spot of the previous assessments. Both quantities and locations were different between inspections.

Technical reports of ACI (ACI 228 Committee, 2003, 2013; ACI 437 Committee, 2003) supports these. Using rebound hammer test alone is not appropriate to estimate a strength, since it is sensitive to a test location, the roughness of a surface, and the existence of rebar, etc. Moreover, the bias could be occurred by the differences in apparatuses, skills of inspectors. Consequently, it may be safely be said that the current assessment methodologies draw a futile result.

Figure 3.8 shows the example of load rating result when the presumed compressive strengths are adopted.

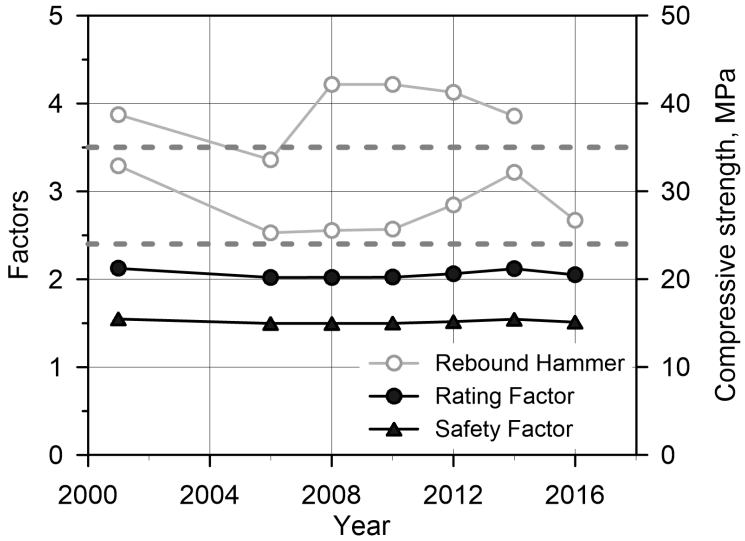

Figure 3.8: Load rating results for case 8 adopting the records of estimated compressive strength; each dashed line refers to the specified strength of deck and girder concrete

Case 8 has the largest differences in strengths when it is compared to the

design strength. The changes were 5.3~33.8% and -4.0~20.4% for deck and girder, respectively. However, the changes in SF and RF were 0.08 and 0.14 in range, respectively.

Therefore, it has been concluded that the current inspection method of presuming strength may be worthless. A reasonable approach for the rebound hammer test is to compare rebound values between sound and unsound area; such as repaired and deteriorated area to check the quality of repair. Otherwise, the test will be just a time-consuming, inefficient task.

3.2.2 Carbonation Depth Measurement

Four cases were examined here. They are the cases that records of carbonation depths and remaining depths exist and their condition rating have been changed. Figure 3.9 shows the records of carbonation depth measurements of the cases. The test results from girders are excluded because of the lack of data. The results are shown in both measured and remaining depths since the condition rating is based on these data. As seen in the previous clause, there were no trends in carbonation depths. The remarkable result was that the ranges of changes in measured depth and remaining depth were not similar. It implies that the cover depths which were referred in determining remaining depth have been changed.

Specifically, for one bridge, some reports used design value while others used measured cover depth. In addition, testing locations had been changed in every assessment. Consequently, the test will not yield consistent evaluations about carbonation conditions.

Figure 3.10 refers the conditional safety and durability performance rating evaluated according to Tables 2.5 and 2.7. While the condition ratings were between a and c, durability performances were evaluated in a for all cases.

Evaluating a conditional safety with changing referred concrete cover might

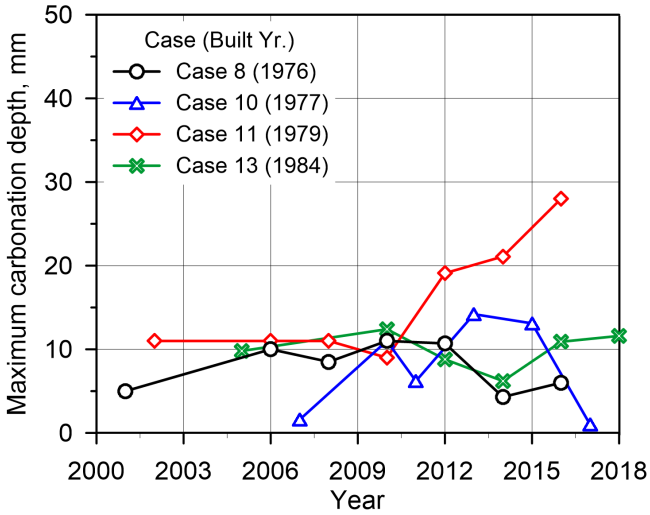

(a) Measured depth

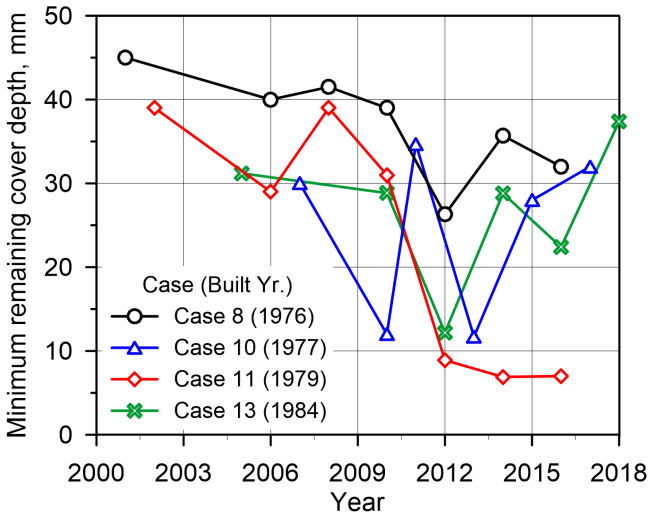

(b) Remaining cover

Figure 3.9: Records of carbonation depth measurement from the data in collected inspection reports; only test results on decks are presented

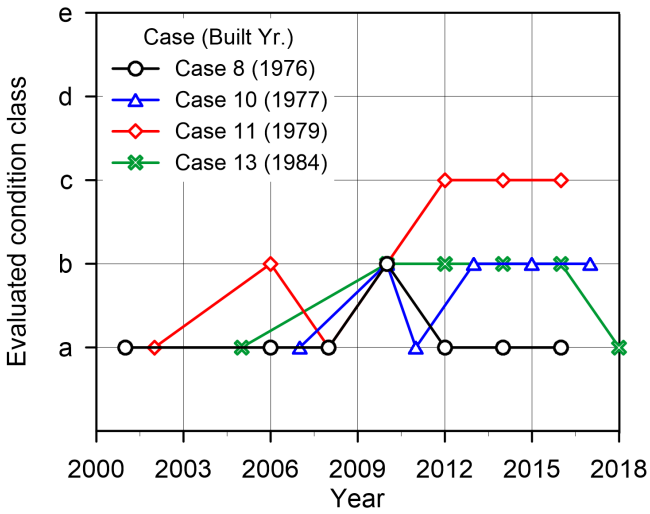

(a) Conditional safety

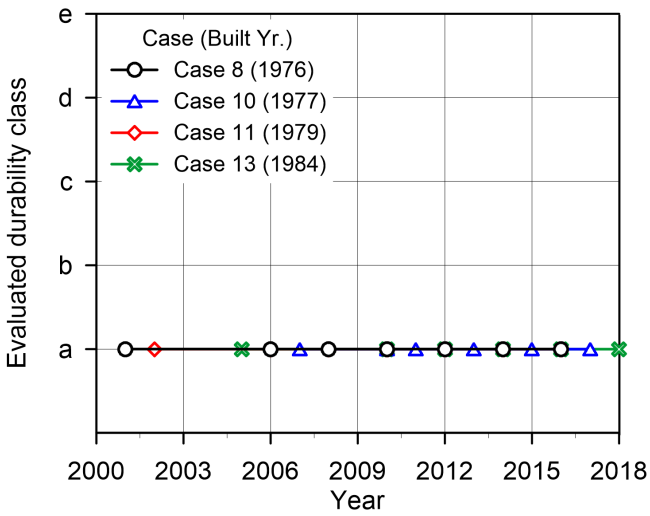

(b) Durability performance

Figure 3.10: Records of rating based on carbonation depth measurement

result in inconsistent results. Hence, it may conclude that the current condition evaluation is not reliable. For a consistent and accurate evaluation, the actual cover depth should be measured, and the testing needs to be conducted in a similar part repeatedly.

One of the current material tests' problems is that the tests have been conducted on the exterior of components. Hence, conditions in material aspects are evaluated only by soundness of materials composing exterior parts. Therefore, the necessities of the tests and validity of evaluation methods need to be confirmed through experimental researches on testing interior of components.

Chapter 4 Conclusions

The thesis set out to examine the validity of the performance assessment guideline for an existing concrete bridge which is implemented in the current inspections.

For a validity analysis, the domestic and foreign assessment guidelines were investigated. The study found that only the Korean guideline specifies the rating method for each inspection item and every component and whole establishment. And the criteria for rating an on-site inspection or a material test are too quantitative and according to these, there have not been engineers' decisions in evaluating structures. It may have led an inefficient assessment of Korea.

The second major finding was that the load rating method of Korea would lead a conservative evaluation. When it is compared to the other guidelines, it provides the large value of live load factor which is the same with that in the former design code. The guideline does not allow a low uncertainty in live load.

To verify the findings, case studies about load rating method and material test were made. Assessment reports and relevant documents of concrete bridges' cases were collected for these. The investigation of load rating based on the original design load of a case showed that the Korean guideline evaluates structural safety most conservatively, in terms of safety factor and rating factor. Load rating based on the design load proposed in each guideline provided a similar level of safety between the inventory level of AASHTO MBE, the design level of KECRI, and the current Korean guideline; while the operating level and permissible level provided a larger value of rating factor.

From the findings the study concluded that the reliability-based load rating

methods could be adopted for an efficient assessment, allowing enough reliable level of safety at the same time.

The study also checked the validity of a diagnostic load test by the actual tests on a flyover bridge. The test did not yield consistent results and it implies that the load test could be worthless in evaluating girder stiffness changes. In further researches, the findings are closely examined through the experimental verification on a decommissioned bridge.

The thesis also has shown inefficiencies of current conditional evaluation methods focusing on material tests through tracing test data. Locations of tests and references to compare with the data were inconsistent in every inspection. Also, the bias from the test apparatus and an inspector's skill contributed to the inconsistencies. From the observations, the study concluded that the current methods of on-site material tests and their evaluation method could be worthless. To improve, ones should be conducted in the same spot, and not for evaluating conditions of a component. Rebound hammer test, for instance, could be conducted to compare the qualities between sound and unsound area.

A limitation of this study is that the conclusions should be experimentally verified for accurate evaluation of each item. It is expected to be verified through specimens from decommissioned bridges, in the further researches. Notwithstanding these limitations, these findings contribute to the understanding of the problems in the current performance assessment methodologies by providing analyses about the actual cases that have been performed in Korea.

Appendix A Load Rating Computation Examples

A.1 Case 4: PSC I Beam Simple Span Bridge

A.1.1 Bridge Data

Span:	29.9 m (Total length: 210.0 m)
Year Built:	1968
Condition Rating:	C
Concrete:	f_{ck} = 27 MPa (Deck)
	f_{ck} = 35 MPa (P/S Beam)
	f_{ck} = 30 MPa (P/S Beam at transfer)
Prestressing Steel:	twelve 7 mm diameter steel wires per each tendon
	A_p = 461.8 mm^2 for each tendon (Assumption)
	f_{pu} = $1,600$ MPa, f_{py} = $1,350$ MPa (Assumption)
	f_{pj} = $0.9 \times 0.85 \times f_{pu}$ (Assumption)
	f_{pe} = 903 MPa at the center
Reinforcing Steel:	Tension, Compression: D13 (126.7 mm^2, f_y = 240 MPa)
Effective Flange Width:	Minimum of
	i) $L/4$
	ii) $12t_s$ + greater of either t_w or $b_{f,top}/2$
	iii) S
	i) (29,900)/4 = 7,475 mm
	ii) $12 \times 200 + 800/2$ = 2,800 mm
	iii) 1,450 mm Governs

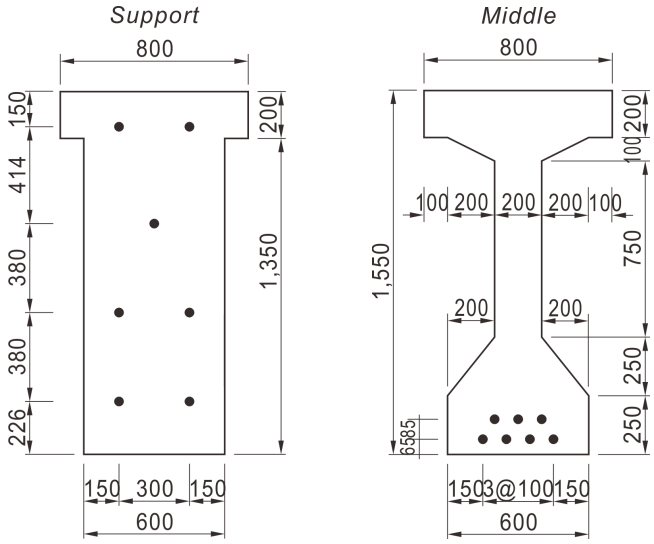

Figure A.1: Section profile of the case 4 beam at its support and center; concrete section and P/S steels are presented

A.1.2 Summary of Section Properties

Beam Section		Composite Section	
h_b	= 1,550 mm	t_s	= 200 mm
A_b	= 617,000 mm^2	A_c	= 907,000 mm^2
I_b	= 1.8269×10^{11} mm^4	I_c	= 3.2864×10^{11} mm^4
Y_b	= 757 mm	Y_c	= 683 mm
S_{bot}	= 2.3046×10^8 mm^3	S_{bot}	= 3.0805×10^8 mm^3
S_{top}	= 2.4125×10^8 mm^3	S_{top}	= 4.8105×10^8 mm^3

A.1.3 Nominal Flexural Resistance at Midspan

Every longitudinal reinforcing steel is considered. The material models for reinforcing steel and P/S steel are assumed to be bi-linear relationship. The total area P/S steels are assumed to be concentrated at the center of all P/S steels (d_p = 1,649 mm). ACI 318 (ACI 318 Committee, 2014) result is presented here.

Strain Compatibility Analysis:

1. Strain on P/S steel due to effective prestress:

$$\varepsilon_1 = \frac{f_{pe}}{E_s} = \frac{903}{200{,}000} = 0.0045$$

2. Decompression:

$$\varepsilon_2 = \frac{\sum A_p f_{pe}}{E_b A_b}\left(1 + \frac{e_p^2}{r_b^2}\right) = \frac{(3{,}232)(903)}{(27{,}804)(617{,}000)}\left(1 + \frac{892^2}{544^2}\right) = 4.4455 \times 10^{-4}$$

3. Strain at failure:

   $\varepsilon_3 = 0.0261$ by iteration, with an error of 2.9129×10^{-8}

4. According distance from the neutral axis to the top fiber is: $c = 185$ mm

Nominal flexural Resistance at midspan is:

$$M_n = M_s + M_p - M_c$$
$$= \sum_i A_{s,i} f_{s,i} + \sum_i A_{p,i} f_{ps} - \int_{A_c} y f_c dA = 558 + 8{,}041 - 425 = 8{,}173 \text{ kN-m}$$

Here, M_c, M_s and M_p refer to moment on concrete, steel, and P/S steel at failure. Adopting provisions in KHBDC (MOLIT, 2016b) and Eurocode 2 (CEN, 2005), design resistances M_d can be calculated as the procedure above.

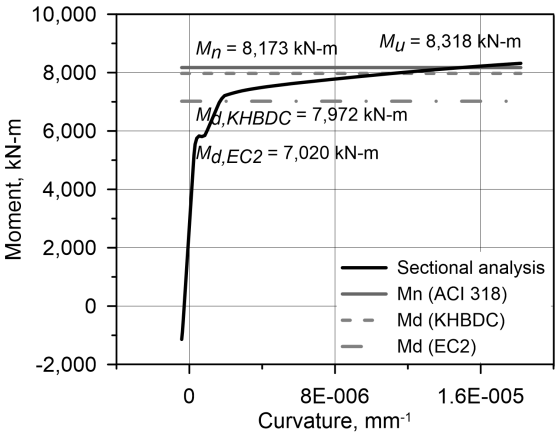

Figure A.2: The flexural resistance computed according to each design code, and the sectional analysis result of the case 4

A.1.4 Load Effects

Dead Load Effect

Detailed drawings for wearing surface and barriers, etc. are not available, and not considered in here. All weights of haunches and lateral beams are considered.

Dead load effect: M_{DC} = 2486 kN-m

Live Load Effect

Live load distribution factor, g_m of AASHTO LRFD (AASHTO, 2017):

K_g = $n(I + Ae_g^2)$

n = $\frac{E_b}{E_d}$ = $\frac{27{,}804}{25{,}500}$ = 1.09

A = 617,000 mm^2

I = 1.8269×10^{11} mm^4

L = 29.9 m

t_s = 200 mm

e_g = girder depth - Y_b + $t_s/2$ = (1,550 - 757) + 200/2 = 893 mm

K_g = 7.3537×10^{11} mm^4

$\frac{K_g}{Lt_s^3}$ = $\frac{7.3537 \times 10^{11}}{(29{,}900)(200)^3}$ = 3.07

Accordingly,

$$g_{m1} = 0.06 + \left(\frac{S}{4{,}300}\right)^{0.4}\left(\frac{S}{L}\right)^{0.3}\left(\frac{K_g}{Lt_s^3}\right)^{0.1} = 0.06 + \left(\frac{1{,}450}{4{,}300}\right)^{0.4}\left(\frac{1{,}450}{29{,}900}\right)^{0.3}(3.07)^{0.1}$$

$$= 0.3522$$

$$g_{m2} = 0.075 + \left(\frac{S}{2{,}900}\right)^{0.6}\left(\frac{S}{L}\right)^{0.2}\left(\frac{K_g}{Lt_s^3}\right)^{0.1} = 0.075 + \left(\frac{1{,}450}{2{,}900}\right)^{0.6}\left(\frac{1{,}450}{29{,}900}\right)^{0.2}(3.07)^{0.1}$$

$$= 0.4780 \quad \text{Governs}$$

$$g_m = 0.4780$$

Live load effect according to each guideline is as follows. Since impact allowance is not considered for a design lane load, load effects of KL-510 and HL-93 below are

computed with the design lane loads multiplied by reciprocal of impact factors. Here, x denotes the distance from the support closest to the front wheel of design truck:

1. DB-24/DL-24 Design Load
   - Design truck moment = 2,743 kN-m Governs
     Maximum moment at x = 14.25 m, front wheel at x = 10.05 m & V = 4.2 m
   - Design lane load moment = 2,227 kN-m
     Maximum moment at midspan
2. KL-510 Design Load
   - Design truck moment = 2,953 kN-m
     Maximum moment at x = 13.95 m, front wheel at x = 9.15 m
   - 0.75×Design truck + Design lane load moment = 3,307 kN-m Governs
     Maximum moment at x = 14.2 m, front wheel at x = 9.40 m
3. HL-93 Design Load
   - Design truck + Design lane load moment = 2,840 kN-m Governs
     Maximum moment at x = 14.40 m, front wheel at x = 10.2 m & V = 4.2 m
   - Design tandem + Design lane load moment = 2,426 kN-m
     Maximum moment at midspan

Dynamic load allowance

Factored load effects are as follows. For guidelines, KISTEC (KISTEC, 2018a; 2018b), AASHTO MBE (AASHTO, 2013) and KECRI (KECRI, 2013), the dynamic load allowances (impact factor) are as follows:

- KISTEC and LFR of AASHTO MBE: i = 0.215
- LRFR of AASHTO MBE: 33% dynamic load allowance
- KECRI: 25% dynamic load allowance

A.1.5 Load Rating According to Guidelines

According to Table 2.22, condition factor for LRFR of AASHTO MBE, BD 21/01, and KECRI is: φ_c = 0.95. Assessment resistance (φM_n or M_d), factored load effect and load rating results are as follows:

Table A.1: Load rating results of the case 4

Guideline	**Assessment Resistance, kN-m**	**Factored Load Effect, kN-m**		$\boldsymbol{SF}$ **or** $\boldsymbol{RF}$
		Dead Load	**Live Load**	
KISTEC	6,947	3,232	3,423	SF = 1.04 RF = 1.09
ACI 562 Min.	7,356	2,983	2,097	SF = 1.45
ACI 562 Max.	8,173			SF = 1.61
BD 21/01	7,020	3,158	2,163	SF = 1.38
KECRI Design	7,573	3,107	3,220	SF = 1.20 RF = 1.40
KECRI Permissible			2,568	SF = 1.33 RF = 2.10
LRFR Inventory	7,764	3,107	3,159	RF = 1.47
LRFR Operating			2,437	RF = 1.91
LFR Inventory	8,173	3,232	3,455	RF = 1.43
LFR Operating			2,070	RF = 2.39

A.2 Case 8: PSC I Beam Simple Span Bridge

A.2.1 Bridge Data

Span:	28.4 m (Total length: 178.5 m)
Year Built:	1976
Condition Rating:	B
Concrete:	f_{ck} = 27 MPa (Deck)
	f_{ck} = 40 MPa (P/S Beam)
	f_{ck} = 30 MPa (P/S Beam at transfer)
Prestressing Steel:	twelve 7 mm diameter steel wires per each tendon
	A_p = 461.8 mm^2 for each tendon
	f_{pu} = $1,550$ MPa, f_{py} = $1,350$ MPa (Assumption)
	f_{pj} = 57 tonf (Design Value)
	f_{pe} = $1,069$ MPa at the center
Reinforcing Steel:	Tension, Compression: D13 (126.7 mm^2, f_y = 240 MPa)
Effective Flange Width:	Minimum of
	i) $L/4$
	ii) $12t_s$ + greater of either t_w or $b_{f,top}/2$
	iii) S
	i) (28,400)/4 = 7,100 mm
	ii) $12 \times 206 + 580/2$ = 2,762 mm
	iii) 2,200 mm Governs

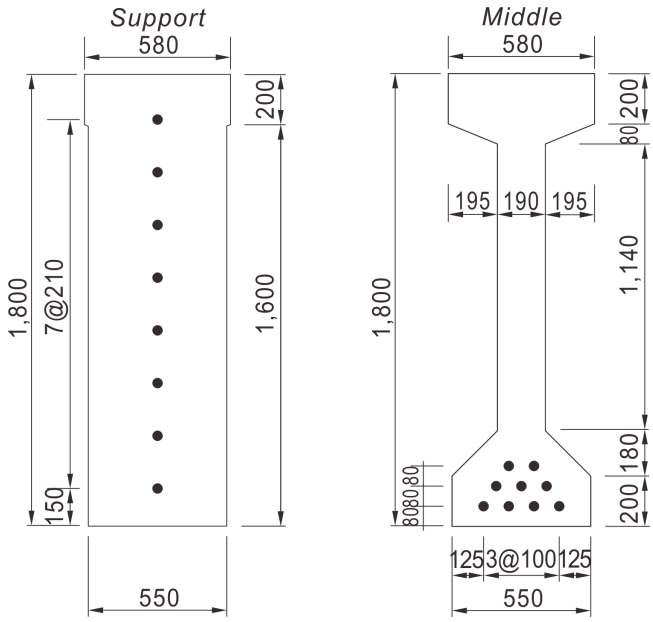

Figure A.3: Section profile of the case 8 beam at its support and center; concrete section and P/S steels are presented

A.2.2 Summary of Section Properties

Beam Section		Composite Section	
h_b	= 1,800 mm	t_s	= 206 mm
A_b	= 545,650 mm^2	A_c	= 998,850 mm^2
I_b	= 2.1380×10^{11} mm^4	I_c	= 4.6931×10^{11} mm^4
Y_b	= 910 mm	Y_c	= 656 mm
S_{bot}	= 2.4014×10^8 mm^3	S_{bot}	= 3.4769×10^8 mm^3
S_{top}	= 2.3502×10^8 mm^3	S_{top}	= 7.1516×10^8 mm^3

A.2.3 Nominal Flexural Resistance at Midspan

Every longitudinal reinforcing steel is considered. The material models for reinforcing steel and P/S steel are assumed to be bi-linear relationship. The total area P/S steels are assumed to be concentrated at the center of all P/S steels (d_p = 1,864 mm). ACI 318

(ACI 318 Committee, 2014) result is presented here.

Strain Compatibility Analysis:

1. Strain on P/S steel due to effective prestress:

$$\varepsilon_1 = \frac{f_{pe}}{E_s} = \frac{1{,}069}{200{,}000} = 0.0053$$

2. Decompression:

$$\varepsilon_2 = \frac{\sum A_p f_{pe}}{E_b A_b}\left(1 + \frac{e_p^2}{r_b^2}\right) = \frac{(4{,}159)(949)}{(29{,}070)(545{,}650)}\left(1 + \frac{954^2}{626^2}\right) = 6.8032 \times 10^{-4}$$

3. Strain at failure:

   $\varepsilon_3 = 0.0350$ by iteration, with an error of 2.9373×10^{-8}

4. According distance from the neutral axis to the top fiber is: $c = 161$ mm

Nominal flexural Resistance at midspan is:

$$\begin{aligned} M_n &= M_s + M_p - M_c \\ &= \sum_i A_{s,i} f_{s,i} + \sum_i A_{p,i} f_{ps} - \int_{A_c} y f_c dA = 769 + 11{,}846 - 495 = 12{,}119 \text{ kN-m} \end{aligned}$$

Here, M_c, M_s and M_p refer to moment on concrete, steel, and P/S steel at failure. Adopting provisions in KHBDC (MOLIT, 2016b) and Eurocode 2 (CEN, 2005), design resistances M_d can be calculated as the procedure above.

A.2.4 Load Effects

Dead Load Effect

Detailed drawings for wearing surface and barriers, etc. are not available, and not considered in here. All weights of haunches and lateral beams are considered.

Dead load effect: M_{DC} = 2,685 kN-m

Live Load Effect

Live load distribution factor, g_m of AASHTO LRFD (AASHTO, 2017):

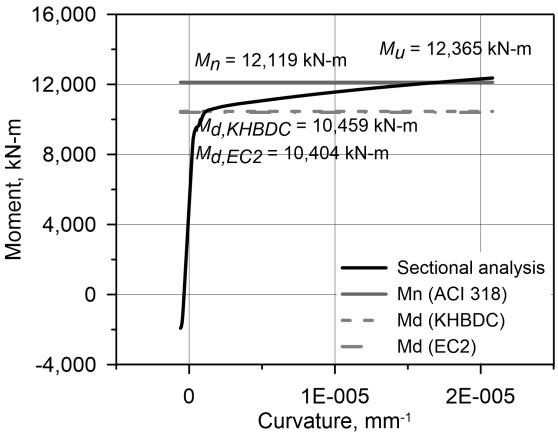

Figure A.4: The flexural resistance computed according to each design code, and the sectional analysis result of the case 8

K_g = $n(I + Ae_g^2)$

n = $\frac{E_b}{E_d}$ = $\frac{29{,}070}{25{,}500}$ = 1.14

A = 545,650 mm^2

I = 2.1380×10^{11} mm^4

L = 28.4 m

t_s = 206 mm

e_g = girder depth - Y_b + $t_s/2$ = (1,800 - 910) + 206/2 = 993 mm

K_g = 8.5744×10^{11} mm^4

$\frac{K_g}{Lt_s^3}$ = $\frac{8.5744 \times 10^{11}}{(28{,}400)(206)^3}$ = 3.45

Accordingly,

$$g_{m1} = 0.06 + \left(\frac{S}{4{,}300}\right)^{0.4}\left(\frac{S}{L}\right)^{0.3}\left(\frac{K_g}{Lt_s^3}\right)^{0.1} = 0.06 + \left(\frac{2{,}200}{4{,}300}\right)^{0.4}\left(\frac{2{,}900}{28{,}400}\right)^{0.3}(3.45)^{0.1}$$

$$= 0.4619$$

$$g_{m2} = 0.075 + \left(\frac{S}{2{,}900}\right)^{0.6}\left(\frac{S}{L}\right)^{0.2}\left(\frac{K_g}{Lt_s^3}\right)^{0.1} = 0.075 + \left(\frac{2{,}200}{2{,}900}\right)^{0.6}\left(\frac{2{,}200}{28{,}400}\right)^{0.2}(3.45)^{0.1}$$

$= 0.6500$ Governs

$g_m = 0.6500$

Live load effect according to each guideline is as follows. Since impact allowance is not considered for a design lane load, load effects of KL-510 and HL-93 below are computed with the design lane loads multiplied by reciprocal of impact factors. Here, x denotes the distance from the support closest to the front wheel of design truck:

1. DB-24/DL-24 Design Load
   - Design truck moment = 1,936 kN-m Governs
     Maximum moment at x = 13.45 m, front wheel at x = 9.25 m & V = 4.2 m
   - Design lane load moment = 1,533 kN-m
     Maximum moment at midspan
2. KL-510 Design Load
   - Design truck moment = 2,762 kN-m
     Maximum moment at x = 13.20 m, front wheel at x = 8.40 m
   - 0.75×Design truck + Design lane load moment = 3,057 kN-m Governs
     Maximum moment at x = 13.45 m, front wheel at x = 8.65 m
3. HL-93 Design Load
   - Design truck + Design lane load moment = 2,642 kN-m Governs
     Maximum moment at x = 13.65 m, front wheel at x = 9.45 m & V = 4.2 m
   - Design tandem + Design lane load moment = 2,267 kN-m
     Maximum moment at midspan

Dynamic load allowance

Factored load effects are as follows. For guidelines, KISTEC (KISTEC, 2018a; 2018b), AASHTO MBE (AASHTO, 2013) and KECRI (KECRI, 2013), the dynamic load allowances (impact factor) are as follows:

- KISTEC and LFR of AASHTO MBE: i = 0.219
- LRFR of AASHTO MBE: 33% dynamic load allowance
- KECRI: 25% dynamic load allowance

A.2.5 Load Rating According to Guidelines

According to Table 2.22, condition factor for LRFR of AASHTO MBE, BD 21/01, and KECRI is: φ_c = 1.00. Assessment resistance (φM_n or M_d), factored load effect and load rating results are as follows:

Table A.2: Load rating results of the case 8

Guideline	**Assessment Resistance, kN-m**	**Factored Load Effect, kN-m**		$\boldsymbol{SF}$ **or** $\boldsymbol{RF}$
		Dead Load	**Live Load**	
KISTEC	10,301	3,490	3,318	SF = 1.51 RF = 2.05
ACI 562 Min.	10,908	3,222	2,025	SF = 2.08
ACI 562 Max.	12,119			SF = 2.31
BD 21/01	10,404	3,410	2,088	SF = 2.09
KECRI Design	10,459	3,356	4,072	SF = 1.41 RF = 1.76
KECRI Permissible			3,248	SF = 1.58 RF = 3.45
LRFR Inventory	12,119	3,356	4,020	RF = 2.18
LRFR Operating			3,101	RF = 2.83
LFR Inventory	12,119	3,490	3,318	RF = 2.58
LFR Operating			2,006	RF = 4.30

A.3 Case 13: PSC I Beam Simple Span Bridge

A.3.1 Bridge Data

Span:	30.5 m (Total length: 480.0 m)
Year Built:	1984
Condition Rating:	C
Concrete:	f_{ck} = 27 MPa (Deck)
	f_{ck} = 35 MPa (P/S Beam)
	f_{ck} = 27 MPa (P/S Beam at transfer)
Prestressing Steel:	eight 8 mm diameter steel wires per each tendon
	A_p = 502.7 mm^2 for each tendon (Assumption)
	f_{pu} = $1,550$ MPa, f_{py} = $1,350$ MPa (Assumption)
	f_{pj} = $0.7f_{pu}$ (Assumption)
	f_{pe} = 949 MPa at the center
Reinforcing Steel:	Tension, Compression: D16 (198.6 mm^2, f_y = 300 MPa)
Effective Flange Width:	Minimum of
	i) $L/4$
	ii) $12t_s$ + greater of either t_w or $b_{f,top}/2$
	iii) S
	i) (30,500)/4 = 7,625 mm
	ii) $12 \times 250 + 900/2$ = 3,450 mm
	iii) 2,900 mm Governs

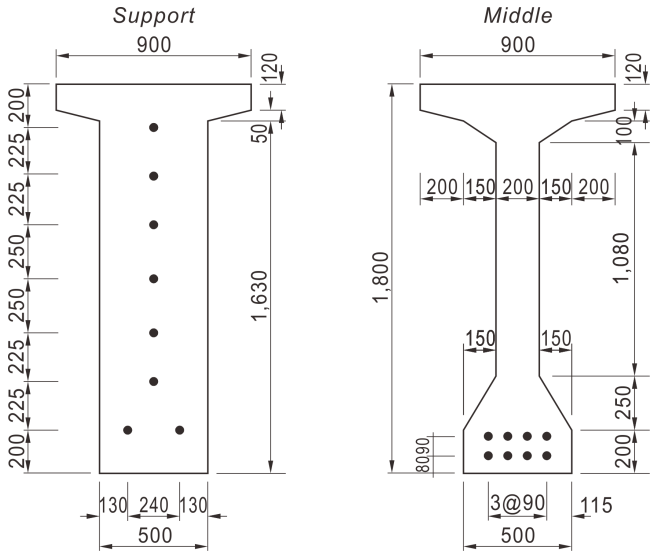

Figure A.5: Section profile of the case 13 beam at its support and center; concrete section and P/S steels are presented

A.3.2 Summary of Section Properties

Beam Section		Composite Section	
h_b	= 1,800 mm	t_s	= 250 mm
A_b	= 588,500 mm^2	A_c	= 1,313,500 mm^2
I_b	= 2.3534×10^{11} mm^4	I_c	= 5.4659×10^{11} mm^4
Y_b	= 728 mm	Y_c	= 441 mm
S_{bot}	= 2.1953×10^8 mm^3	S_{bot}	= 1.2394×10^9 mm^3
S_{top}	= 3.2327×10^8 mm^3	S_{top}	= 3.3971×10^8 mm^3

A.3.3 Nominal Flexural Resistance at Midspan

Every longitudinal reinforcing steel is considered. The material models for reinforcing steel and P/S steel are assumed to be bi-linear relationship. The total area P/S steels are assumed to be concentrated at the center of all P/S steels (d_p = 1,805 mm). ACI 318 (ACI 318 Committee, 2014) result is presented here.

Strain Compatibility Analysis:

1. Strain on P/S steel due to effective prestress:

$$\varepsilon_1 = \frac{f_{pe}}{E_s} = \frac{949}{200{,}000} = 0.0047$$

2. Decompression:

$$\varepsilon_2 = \frac{\sum A_p f_{pe}}{E_b A_b}\left(1 + \frac{e_p^2}{r_b^2}\right) = \frac{(4{,}022)(949)}{(27{,}804)(588{,}500)}\left(1 + \frac{1{,}077^2}{632^2}\right) = 6.3231 \times 10^{-4}$$

3. Strain at failure:

   $\varepsilon_3 = 0.0494$ by iteration, with an error of 5.3225×10^{-8}

4. According distance from the neutral axis to the top fiber is: $c = 113$ mm

Nominal flexural Resistance at midspan is:

$$M_n = M_s + M_p - M_c$$
$$= \sum_i A_{s,i} f_{s,i} + \sum_i A_{p,i} f_{ps} - \int_{A_c} y f_c dA = 1{,}255 + 11{,}413 - 333 = 12{,}335 \text{ kN-m}$$

Here, M_c, M_s and M_p refer to moment on concrete, steel, and P/S steel at failure. Adopting provisions in KHBDC (MOLIT, 2016b) and Eurocode 2 (CEN, 2005), design resistances M_d can be calculated as the procedure above.

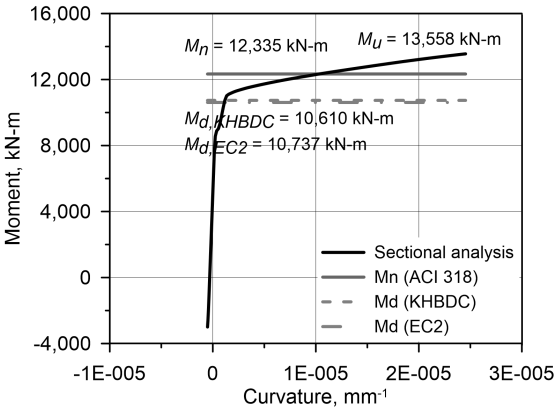

Figure A.6: The flexural resistance computed according to each design code, and the sectional analysis result of the case 13

A.3.4 Load Effects

Dead Load Effect

Detailed drawings for wearing surface and barriers, etc. are not available, and not considered in here. All weights of haunches and lateral beams are considered.

Dead load effect: M_{DC} = 3,537 kN-m

Live Load Effect

Live load distribution factor, g_m of AASHTO LRFD (AASHTO, 2017):

K_g = $n(I + Ae_g^2)$

n = $\frac{E_b}{E_d}$ = $\frac{27{,}804}{25{,}500}$ = 1.09

A = 588,500 mm^2

I = 2.3534×10^{11} mm^4

L = 30.5 m

t_s = 250 mm

e_g = girder depth - Y_b + $t_s/2$ = (1,800 - 728) + 250/2 = 1,077 mm

K_g = 1.0010×10^{12} mm^4

$\frac{K_g}{Lt_s^3}$ = $\frac{1.0010 \times 10^{12}}{(30{,}500)(250)^3}$ = 2.10

Accordingly,

$$g_{m1} = 0.06 + \left(\frac{S}{4{,}300}\right)^{0.4}\left(\frac{S}{L}\right)^{0.3}\left(\frac{K_g}{Lt_s^3}\right)^{0.1} = 0.06 + \left(\frac{2{,}900}{4{,}300}\right)^{0.4}\left(\frac{2{,}900}{30{,}500}\right)^{0.3}(2.10)^{0.1}$$

$$= 0.5142$$

$$g_{m2} = 0.075 + \left(\frac{S}{2{,}900}\right)^{0.6}\left(\frac{S}{L}\right)^{0.2}\left(\frac{K_g}{Lt_s^3}\right)^{0.1} = 0.075 + \left(\frac{2{,}900}{2{,}900}\right)^{0.6}\left(\frac{2{,}900}{30{,}500}\right)^{0.2}(2.10)^{0.1}$$

$$= 0.7477 \quad \text{Governs}$$

$$g_m = 0.7477$$

Live load effect according to each guideline is as follows. Since impact allowance is not considered for a design lane load, load effects of KL-510 and HL-93 below are

computed with the design lane loads multiplied by reciprocal of impact factors. Here, x denotes the distance from the support closest to the front wheel of design truck:

1. DB-24/DL-24 Design Load
   - Design truck moment = 2,807 kN-m Governs
     Maximum moment at x = 14.50 m, front wheel at x = 10.3 m & V = 4.2 m
   - Design lane load moment = 2,300 kN-m
     Maximum moment at midspan
2. KL-510 Design Load
   - Design truck moment = 3,029 kN-m
     Maximum moment at x = 14.25 m, front wheel at x = 9.45 m
   - 0.75×Design truck + Design lane load moment = 3,408 kN-m Governs
     Maximum moment at x = 14.60 m, front wheel at x = 9.80 m
3. HL-93 Design Load
   - Design truck + Design lane load moment = 2,920 kN-m Governs
     Maximum moment at x = 14.50 m, front wheel at x = 10.3 m & V = 4.2 m
   - Design tandem + Design lane load moment = 2,491 kN-m
     Maximum moment at midspan

Dynamic load allowance

Factored load effects are as follows. For guidelines, KISTEC (KISTEC, 2018a; 2018b), AASHTO MBE (AASHTO, 2013) and KECRI (KECRI, 2013), the dynamic load allowances (impact factor) are as follows:

- KISTEC and LFR of AASHTO MBE: i = 0.213
- LRFR of AASHTO MBE: 33% dynamic load allowance
- KECRI: 25% dynamic load allowance

A.3.5 Load Rating According to Guidelines

According to Table 2.22, condition factor for LRFR of AASHTO MBE, BD 21/01, and KECRI is: φ_c = 0.95. Assessment resistance (φM_n or M_d), factored load effect and load rating results are as follows:

Table A.3: Load rating results of the case 13

Guideline	**Assessment Resistance, kN-m**	**Factored Load Effect, kN-m**		$\boldsymbol{SF}$ **or** $\boldsymbol{RF}$
		Dead Load	**Live Load**	
KISTEC	10,485	4,598	5,473	SF = 1.04 RF = 1.08
ACI 562 Min.	11,101	4,245	3,359	SF = 1.46
ACI 562 Max.	12,335			SF = 1.62
BD 21/01	10,737	4,492	3,464	SF = 1.40
KECRI Design	10,260	4,421	5,192	SF = 1.06 RF = 1.19
KECRI Permissible			4,141	SF = 1.12 RF = 1.69
LRFR Inventory	11,718	4,421	5,082	RF = 1.44
LRFR Operating			3,920	RF = 1.86
LFR Inventory	12,335	4,598	5,524	RF = 1.40
LFR Operating			3,309	RF = 2.34

A.4 Case 14: PSC I Beam Simple Span Bridge

A.4.1 Bridge Data

Span:	14.95 m (Total length: 240.0 m)
Year Built:	1986
Condition Rating:	C
Concrete:	f_{ck} = 27 MPa (Deck)
	f_{ck} = 35 MPa (P/S Beam)
	f_{ck} = 27 MPa (P/S Beam at transfer)
Prestressing Steel:	twelve 7 mm diameter steel wires per each tendon
	A_p = 461.8 mm^2 for each tendon (Assumption)
	f_{pu} = $1,600$ MPa, f_{py} = $1,350$ MPa (Assumption)
	f_{pj} = $0.9 \times 0.85 \times f_{pu}$ (Assumption)
	f_{pe} = 864 MPa at the center
Reinforcing Steel:	Tension, Compression: D13 (126.7 mm^2, f_y = 240 MPa)
Effective Flange Width:	Minimum of
	i) $L/4$
	ii) $12t_s$ + greater of either t_w or $b_{f,top}/2$
	iii) S
	i) (14,950)/4 = 3,738 mm
	ii) $12 \times 200 + 500/2$ = 2,650 mm
	iii) 1,500 mm Governs

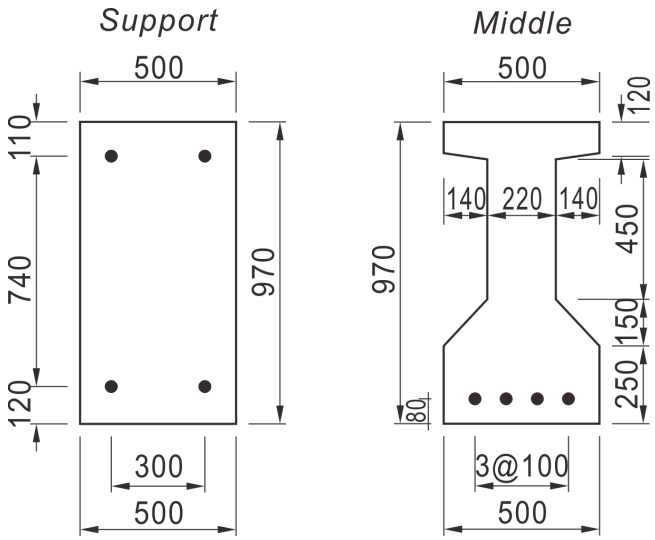

Figure A.7: Section profile of the case 14 beam at its support and center; concrete section and P/S steels are presented

A.4.2 Summary of Section Properties

Beam Section		Composite Section	
h_b	= 970 mm	t_s	= 200 mm
A_b	= 340,200 mm^2	A_c	= 640,200 mm^2
I_b	= 3.3085×10^{10} mm^4	I_c	= 9.7675×10^{10} mm^4
Y_b	= 532 mm	Y_c	= 436 mm
S_{bot}	= 7.5464×10^7 mm^3	S_{bot}	= 1.3300×10^8 mm^3
S_{top}	= 6.2239×10^7 mm^3	S_{top}	= 2.2422×10^8 mm^3

A.4.3 Nominal Flexural Resistance at Midspan

Every longitudinal reinforcing steel is considered. The material models for reinforcing steel and P/S steel are assumed to be bi-linear relationship. The total area P/S steels are assumed to be concentrated at the center of all P/S steels (d_p = 1,090 mm). ACI 318 (ACI 318 Committee, 2014) result is presented here.

Strain Compatibility Analysis:

1. Strain on P/S steel due to effective prestress:

$$\varepsilon_1 = \frac{f_{pe}}{E_s} = \frac{864}{200{,}000} = 0.0043$$

2. Decompression:

$$\varepsilon_2 = \frac{\sum A_p f_{pe}}{E_b A_b}\left(1 + \frac{e_p^2}{r_b^2}\right) = \frac{(1{,}847)(864)}{(27{,}804)(340{,}200)}\left(1 + \frac{558^2}{312^2}\right) = 3.9169 \times 10^{-4}$$

3. Strain at failure:

   $\varepsilon_3 = 0.0255$ by iteration, with an error of 5.5638×10^{-8}

4. According distance from the neutral axis to the top fiber is: $c = 125$ mm

Nominal flexural Resistance at midspan is:

$$M_n = M_s + M_p - M_c$$
$$= \sum_i A_{s,i} f_{s,i} + \sum_i A_{p,i} f_{ps} - \int_{A_c} y f_c dA = 576 + 3{,}027 - 208 = 3{,}395 \text{ kN-m}$$

Here, M_c, M_s and M_p refer to moment on concrete, steel, and P/S steel at failure. Adopting provisions in KHBDC (MOLIT, 2016b) and Eurocode 2 (CEN, 2005), design resistances M_d can be calculated as the procedure above.

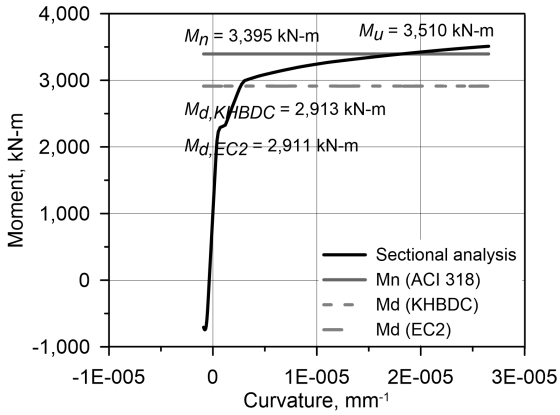

Figure A.8: The flexural resistance computed according to each design code, and the sectional analysis result of the case 14

A.4.4 Load Effects

Dead Load Effect

Detailed drawings for wearing surface and barriers, etc. are not available, and not considered in here. All weights of haunches and lateral beams are considered.

Dead load effect: M_{DC} = 416 kN-m

Live Load Effect

Live load distribution factor, g_m of AASHTO LRFD (AASHTO, 2017):

K_g = $n(I + Ae_g^2)$

n = $\frac{E_b}{E_d}$ = $\frac{27{,}804}{25{,}500}$ = 1.09

A = 340,200 mm^2

I = 3.3085×10^{10} mm^4

L = 14.95 m

t_s = 200 mm

e_g = girder depth - $Y_b + t_s/2$ = (970-532) + 200/2 = 538 mm

K_g = 1.4361×10^{11} mm^4

$\frac{K_g}{Lt_s^3}$ = $\frac{1.4361 \times 10^{11}}{(14{,}950)(200)^3}$ = 1.20

Accordingly,

$$g_{m1} = 0.06 + \left(\frac{S}{4{,}300}\right)^{0.4}\left(\frac{S}{L}\right)^{0.3}\left(\frac{K_g}{Lt_s^3}\right)^{0.1} = 0.06 + \left(\frac{1{,}500}{4{,}300}\right)^{0.4}\left(\frac{1{,}500}{14{,}950}\right)^{0.3}(1.20)^{0.1}$$

$$= 0.3953$$

$$g_{m2} = 0.075 + \left(\frac{S}{2{,}900}\right)^{0.6}\left(\frac{S}{L}\right)^{0.2}\left(\frac{K_g}{Lt_s^3}\right)^{0.1} = 0.075 + \left(\frac{1{,}500}{2{,}900}\right)^{0.6}\left(\frac{1{,}500}{14{,}950}\right)^{0.2}(1.20)^{0.1}$$

$$= 0.5080 \quad \text{Governs}$$

$$g_m = 0.5080$$

Live load effect according to each guideline is as follows. Since impact allowance is not considered for a design lane load, load effects of KL-510 and HL-93 below are

computed with the design lane loads multiplied by reciprocal of impact factors. Here, x denotes the distance from the support closest to the front wheel of design truck:

1. DB-24/DL-24 Design Load
   - Design truck moment = 1,129 kN-m Governs
     Maximum moment at x = 6.75 m, front wheel at x = 2.55 m & V = 4.2 m
   - Design lane load moment = 2,300 kN-m
     Maximum moment at midspan
2. KL-510 Design Load
   - Design truck moment = 1,056 kN-m
     Maximum moment at x = 6.45 m, front wheel at x = 1.65 m
   - 0.75×Design truck + Design lane load moment = 1,061 kN-m Governs
     Maximum moment at x = 6.60 m, front wheel at x = 1.80 m
3. HL-93 Design Load
   - Design truck + Design lane load moment = 1,041 kN-m Governs
     Maximum moment at x = 6.80 m, front wheel at x = 2.60 m & V = 4.2 m
   - Design tandem + Design lane load moment = 1,014 kN-m
     Maximum moment at midspan

Dynamic load allowance

Factored load effects are as follows. For guidelines, KISTEC (KISTEC, 2018a; 2018b), AASHTO MBE (AASHTO, 2013) and KECRI (KECRI, 2013), the dynamic load allowances (impact factor) are as follows:

- KISTEC and LFR of AASHTO MBE: i = 0.273
- LRFR of AASHTO MBE: 33% dynamic load allowance
- KECRI: 25% dynamic load allowance

A.4.5 Load Rating According to Guidelines

According to Table 2.22, condition factor for LRFR of AASHTO MBE, BD 21/01, and KECRI is: φ_c = 0.95. Assessment resistance (φM_n or M_d), factored load effect and load rating results are as follows:

Table A.4: Load rating results of the case 14

Guideline	**Assessment Resistance, kN-m**	**Factored Load Effect, kN-m**		$\boldsymbol{SF}$ **or** $\boldsymbol{RF}$
		Dead Load	**Live Load**	
KISTEC	2,886	541	1,578	SF = 1.36 RF = 1.49
ACI 562 Min.	3,056	499	922	SF = 2.15
ACI 562 Max.	3,395			SF = 2.39
BD 21/01	2,765	529	951	SF = 2.06
KECRI Design	2,767	520	1,187	SF = 1.63 RF = 1.90
KECRI Permissible			947	SF = 1.88 RF = 2.40
LRFR Inventory	11,718	520	1,312	RF = 2.06
LRFR Operating			1,012	RF = 2.67
LFR Inventory	12,335	541	1,592	RF = 1.79
LFR Operating			954	RF = 2.99

A.5 Summary of Examined Sections

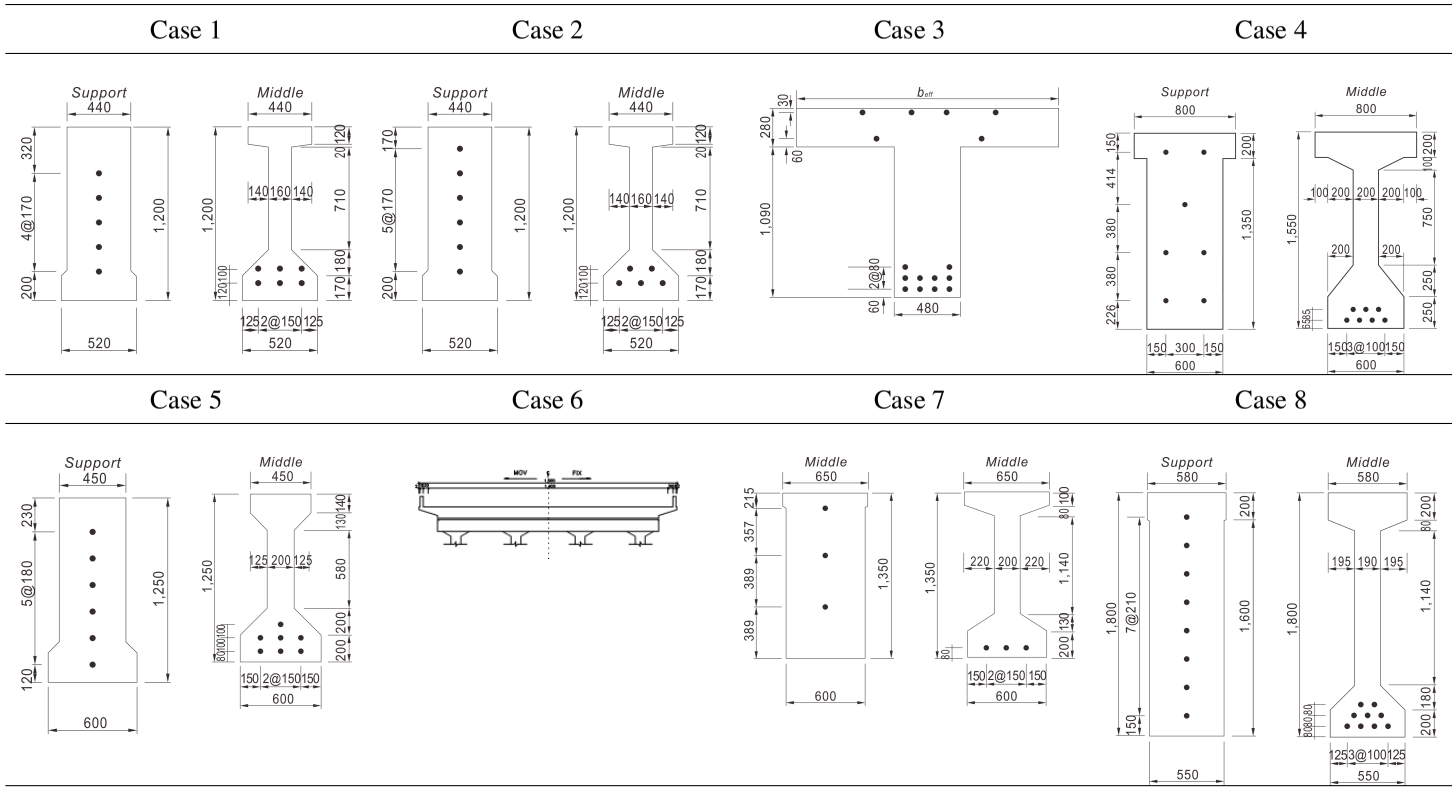

Case 9

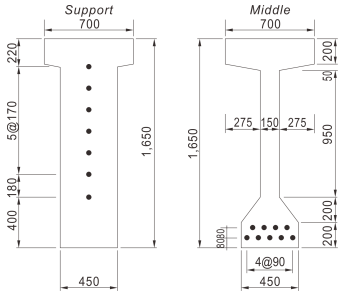

Case 10

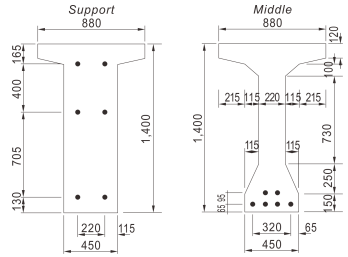

Case 11

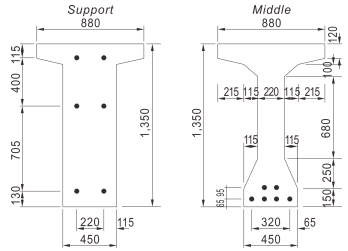

Case 12

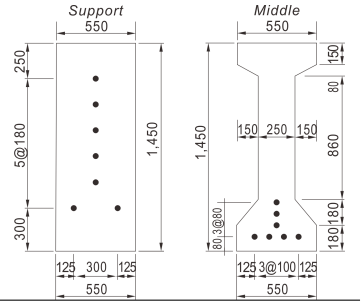

Case 13

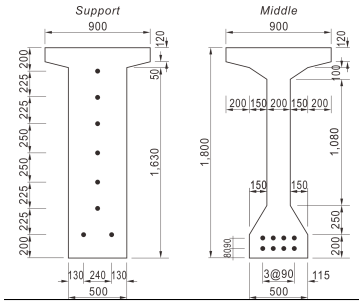

Case 14

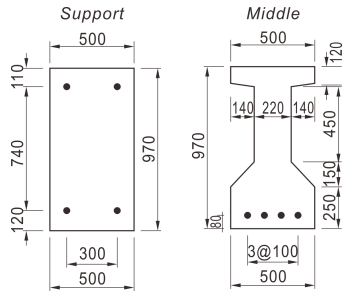

References

ACI 228 Committee. (2003). *In-Place MEthods to Estimate Concrete Strength (ACI 228.1R-03*. American Concrete Institute.

ACI 228 Committee. (2013). *Report on Nondestructive Test Methods for Evaluation of Concrete in Structures (ACI 228.2R-13)*. American Concrete Institute.

ACI 318 Committee. (2014). *Building Code Requirements for Structural Concrete (ACI 318-14) and Commentary*. Farmington Hills, MI: American Concrete Institute.

ACI 437 Committee. (2003). *Strength Evaluation of Existing Concrete Buildings (ACI 437R-03)*. American Concrete Institute.

ACI 562 Committee. (2016). *Code Requirements for Assessment, Repair, and Rehabilitation of Existing Concrete Structures (ACI 562-16) and Commentary*. Farmington Hills, MI: American Concrete Institute.

Almusallam, A., Al-Gahtani, A., Aziz, A., & Rasheeduzzafar. (1996). Effect of reinforcement corrosion on bond strength. *Construction and Building Materials*, *10*(2), pp. 123-129.

Al-Sulaimani, G., Kaleemullah, M., Basunbul, I., & Rasheeduzzafar. (1990). Influence of corrosion and cracking on bond behaviour and strength of reinforced concrete members. *ACI Structural Journal*, *87*(2), pp. 220-231.

American Association of State Highway and Transportation Officials (AASHTO). (1994). *AASHTO Manual for Condition Evaluation of Bridges*. Washington, DC: AASHTO.

American Association of State Highway and Transportation Officials (AASHTO). (2002). *AASHTO Standard Specifications for Highway Bridges* (8th ed.). Washington, DC: AASHTO.

American Association of State Highway and Transportation Officials (AASHTO). (2013). *AASHTO The Manual for Bridge Evaluation* (2nd ed.). Washington, DC: AASHTO.

American Association of State Highway and Transportation Officials (AASHTO). (2017). *AASHTO LRFD Bridge Design Specifications* (17th ed.). Washington, DC: AASHTO.

Andrade, C., Alonso, C., & Molina, F. (1993). Cover cracking as a fuction of bar corrosion: Part 1-experimental test. *Materials and Structures*, *26*, pp. 453-464.

Auyeung, Y., Balaguru, P., & Chung, L. (2000). Bond behavior of corroded reinforcement bars. *ACI Materials Journal*, *97*(2), pp. 214-221.

Bangert, F., Kuhl, D., & Meschke, G. (2004). Chemo-hygro-mechanical modelling and numerical simulation of concrete deterioration caused by alkali-silica reaction. *Journal for Numerical and Analytical Methods in Geomechanics*, *28*, pp. 689-714.

Basheer, P., Chidac, S., & Long, A. (1996). Predictive models for deterioration of concrete structures. *Construction and Building Materials*, *10*(1), pp. 27-37.

Bhargava, K., Ghosh, A., Mori, Y., & Ramanujam, S. (2005). Modeling of time to corrosion-induced cover cracking in reinforced concrete structures. *Cement and Concrete Researches*, *35*, pp. 2203-2218.

Bhargava, K., Ghosh, A., Mori, Y., & Ramanujam, S. (2007). Corrosion-induced bond strength degradation in reinforced concrete-analytical and empirical models. *Nuclear Engineering and Design*, *237*, pp. 1140-1157.

Cabrera, J. (1996). Deterioration of concrete due to reinforcement steel corrosion. *Cement & Concrete Composites*, *18*, pp. 47-59.

Castel, A., Khan, I., Francois, R., & Gilbert, R. (2016). Modeling steel concrete bond strength reduction due to corrosion. *ACI Structural Journal*, *113*(5), pp. 973-982.

Chen, D., & Mahadevan, S. (2008). Chloride-induced reinforcement corrosion and concrete cracking simulation. *Cement & Concrete Composites*, *30*, pp. 227-238.

Chungnam National University. (2002). *A Proposal of Presumption Equation for High Strength Concrete Strength* (Tech. Rep.). Ministry of Commerce Industry and Energy (in Korean).

Coronelli, D., Castel, A., Vu, N., & Francois, R. (2009). Corroded post-tensioned beams with bonded tendons and wire failure. *Engineering Structures*, *31*, pp. 1687-1697.

European Committee for Standardization (CEN). (2005). *Eurocode 2: Design of Concrete Structures - Part 2: Concrete Bridges - Design and Detailing Rules*. Brussels: CEN.

Fang, C., Lundren, K., Plos, M., & Gylltoft, K. (2006). Bond behaviour of corroded reinforcing steel bars in concrete. *Cement and Concrete Researches*, *36*, pp. 1931-3938.

Federal Highway Administration (FHWA). (1995). *Recording and Coding Guide for the Structure Inventory and Appraisal of the Nation's Bridges*. Washington, DC: FHWA.

Gao, R., Li, Q., & Zhao, S. (2013). Concrete deterioration mechanisms under combined sulfate attack and flexural loading. *Journal of Materials in Civil Engineering*, *25*(1), pp. 39-44.

Goltermann, P. (1994a). Mechanical predictions on concrete deterioration. part

1: Eigenstresses in concrete. *ACI Materials Journal*, *91*(6), pp. 543-550.

Goltermann, P. (1994b). Mechanical predictions on concrete deterioration. part 2: Classification of crack patterns. *ACI Materials Journal*, *92*(1), pp. 58-62.

Guo, T., Frangopol, D., Han, D., & Chen, Y. (2011). Probabilistic assessment of deteriorating prestressed concrete box-girder bridges under increased vehicle loads and aggressive environment. *Journal of Performance of Constructed Facilities*, *25*(6), pp. 564-576.

Han, S.-J., Lee, D., Kim, K., Seo, S.-Y., & Moon, J. (2014). Degradation of flexural strength in reinforced concrete members caused by steel corrosion. *Construction and Building Materials*, *54*, pp. 572-583.

Hwang, E.-S., Nguyen, T., & Kim, D.-Y. (2013). Load factors for reliability-based bridge evaluation. *KSCE Jorunal of Civil Engineeing*, *17*(3), pp. 499-508.

Ichikawa, T., & Miura, M. (2007). Modified model of alkali-silica reaction. *Cement and Concrete Researches*, *37*, pp. 1291-1297.

Ju, M., Park, K., & Oh, H. (2017). Estimation of compressive strength of high strength concrete using non-destructive technique and concrete core strength. *Applied Science*, *7*(1249).

Korea Concrete Institute (KCI). (2012). *Korea Structural Concrete Design Code 2012*. Seoul: KCI.

Korea Expressway Corporation Research Institute (KECRI). (2013). *Reliability-Based Safety Assessment Guidelines of Expressway Bridges*. Hwaseong, Korea: Korea Expressway Corporation (in Korean).

Korea Infrastructure Safety and Technology Corporation (KISTEC). (1995). *Detailed Guidelines for Safety Inspection and Full Safety Examination*. Seoul: KISTEC (in Korean).

Korea Infrastructure Safety and Technology Corporation (KISTEC). (2018a). *Detailed Guidelines for Safety Control and Maintenance of Establishments (Performance Evaluation)*. Jinju: KISTEC (in Korean).

Korea Infrastructure Safety and Technology Corporation (KISTEC). (2018b). *Detailed Guidelines for Safety Control and Maintenance of Establishments (Safety Inspection & Examination)*. Jinju: KISTEC (in Korean).

Korea Institute of Civil Engineering and Building Technology (KICT). (2017). *Yearbook of Road Maintenance*. Retrieved December 5, 2018, from http://www.rsis.kr/notify_notice_list.htm/

Korea Institute of Civil Engineering and Building Technology (KICT). (2018, July). *Highway Bridge and Tunnel Information System.* Retrieved November 19, 2018, from https://bti.kict.re.kr/bti/

Kwon, Y.-W., Park, S.-C., & Kim, M.-S. (2006). Strength prediction equations for high strength by schmidt hammer test. *Journal of the Korea Concrete Institute*, *18*(3), pp. 389-395 (in Korean).

Lee, H.-S., Noguchi, T., & Tomosawa, F. (2002). Evaluation of the bond properties beween concrete and reinforcement as function of the degree of reinforcement corrosion. *Cement and Concrete Researches*, *32*, pp. 1313-1318.

Li, C.-Q. (2003). Life-cycle modeling of corrosion-affected concrete structures: Propagation. *Journal of Structural Engineering*, *129*(6), pp. 753-761.

Li, C.-Q., Melchers, R., & Zheng, J.-J. (2006). Analytical model for corrosion-induced crack width in reinforced concrete structures. *ACI Structural Journal*, *103*(4), pp. 479-487.

Li, F., Yuan, Y., & Li, C.-Q. (2011). Corrosion propagation of prestressing steel strands in cocnrete subject to chloride attack. *Construction and Building Materials*, *25*, pp. 3878-3885.

Liu, Y., & Weyers, R. (1998). Modeling the time-to-corrosion cracking in chloride contaminated renforced concrete structures. *ACI Materials Journal*, *95*(6), pp. 675-681.

Lundren, K. (2002). Modelling the effect of corrosion on bond in reinforced concrete. *Magazine of Concrete Researche*, *54*(3), pp. 165-173.

Maaddawy, T., & Soudki, K. (2007). A model for prediction of time from corrosion inititaion to corrosion cracking. *Cement & Concrete Composites*, *29*, pp. 168-175.

Minervino, C., Sivakumar, B., Moses, F., Mertz, D., & Edberg, W. (2004). New aashto guide manual for load and resistance factor rating of highway bridges. *Journal of Bridge Engineering*, *9*(1), pp. 43-54.

Ministry of Land, Infrastructure and Transportation (MOLIT). (2016a). *Handbook of Road Work*. Retrieved December 5, 2018, from http://www.molit.go.kr/USR/BORD0201/m_34879/DTL.jsp?mode=view&idx=30202/

Ministry of Land, Infrastructure and Transportation (MOLIT). (2016b). *Korea Highway Bridge Design Code (Limit State Design)*. Sejong: MOLIT (in Korean).

Ministry of Land, Transport and Maritime Affairs (MLTM). (2010). *Korea Highway Bridge Design Code*. Seoul: MLTM (in Korean).

Molina, F., Alonso, C., & Andrade, C. (1993). Cover cracking as a fuction of bar corrosion: Part 2-numerical model. *Materials and Structures*, *26*, pp. 532-548.

National Bridge Inspection Standards, 74 FR 68377. (December 24, 2009). (to be codified at 23 C.F.R. pts 650). Retrieved from https://www.govinfo.gov/content/pkg/FR-2009-12-24/pdf/E9-30469.pdf

Pantazopoulou, S., & Papoulia, K. (2001). Modeling cover-cracking due to reinforcement corrosion in rc structures. *Journal of Engineering Mechanics*,

127(4), pp. 342-351.

Piast, W., & Schneider, U. (1992). Deformations and elastic modulus of concrete under sustained compression and sulphate attack. *Cement and Concrete Researches*, *22*, pp. 149-158.

Saetta, A. (2005). Deterioration of reinforced structures due to chemical-physical phenomena: Model-based simulation. *Journal of Materials in Civil Engineering*, *17*(3), pp. 313-319.

Seoul National University. (1998). *Development of Strength Evaluation Techniques of Concrete Structures by Nondestructive Test* (Tech. Rep.). Ministry of Science and Technology (in Korean).

Shodja, H., Kiani, K., & Hashemian, A. (2010). A model for the evolution of concrete deterioration due to reinforcement corrosion. *Mathematical and Computer Modelling*, *52*, pp. 1403-1422.

Special Act on the Safety Control of Public Structures, Act No. 4922. (Jan. 5, 1995). (kor). Retrieved from https://elaw.klri.re.kr/kor_service/lawView.do?lang=ENG&hseq=6982

The Highways Agency. (2001). *BD 21/01 The Assessment of Highway Bridges and Structures*. London: The Stationery Office.

The Highways Agency. (2015). *BD 44/15 The Assessment of Concrete Highway Bridges and Structures*. London: The Stationery Office.

Thomas, W., Eric, J., Chill, Z., & Bryan, T. (2012). *Bridge Inspector's Reference Manual (BIRM)*. Moon Township, PA: Federal Highway Administration (FHWA).

Tuutti, K. (1980). Service life of structures with regard to corrosion of embedded steel. *ACI Special Publication (SP 65-13)*, pp. 223-226.

Tuutti, K. (1982). *Corrosion of Steel in Concrete*. Stockholm: Swedish Cement and Concrete Research Institute.

Vidal, T., Castel, A., & Francois, R. (2004). Analyzing crack width to predict corrosion in reinforced concrete. *Cement and Concrete Researches*, *34*, pp. 165-174.

Vu, N., Castel, A., & Francois, R. (2009). Effect of stress corrosion cracking on stress-strain response of steel wires used in prestressed concrete beams. *Corrosion Science*, *51*, pp. 1453-1459.

Wang, L., Zhang, X., Zhang, J., Ma, Y., Xiang, Y., & Liu, Y. (2014). Effect of insufficient grouting and strand corrosion on flexural behavior of pc beams. *Construction and Building Materials*, *53*, pp. 213-224.

Wang, N., Ellingwood, B., Zureick, A.-H., & O'Malley, C. (2009). *Report of Task 1-Appraisal of State-of-the-Art of Bridge Condition Assessment: Condition Assessment of Existing Bridge Structures* (Tech. Rep.). Georgia Institute of Technology.

Weyers, R. (1998). Service life model for concrete structures in chloride laden environments. *ACI Materials Journal*, *95*(4), pp. 445-451.

국 문 초 록

공용중인 콘크리트 교량의 성능평가 방법 타당성 분석

김 민 영

한국의 경제가 발전함에 따라 80년대 중반부터 교량 건설이 급격히 증가하였다. 특히 콘크리트 교량이 그 대부분을 차지하기 때문에 현재 공용 중인 콘크리트 교량의 정확한 성능평가에 대한 요구가 증가하고 있다. 특히 노후된 콘크리트 교량의 경우, 염화물 침투, 탄산화 등으로 인한 철근 부식 등 눈에 보이지 않는 열화가 진행되기 때문에 이러한 상태와 안전성을 평가, 예측하기 위한 기술개발이 요구되고 있다.

시설물 안전 및 유지관리에 관한 특별법이 1995년에 제정되며 시설물에 대한 안전점검, 진단 등이 의무화되었고, 지금까지 제1종, 제2종 시설물에 대해 주기적으로 평가를 하고 있다. 시설물의 안전점검 및 진단은《시설물 안전 및 유지관리 실시 세부지침》에 따라 수행되며 교량의 안전점검, 진단 또한 이 지침에 의해 수행되고 있다.

그러나 노후 시설물의 상태, 안전성을 정확히 평가할 수 있는지에 대한 문제가 지속적으로 제기되어 왔고 이에 대한 연구가 진행되고 있다. 사용 중 교량의 경제적 성능평가를 위해 성능중심평가 지침이 신설되어 2018년부터

실시되고 있으나 이 또한 기존의 지침과 평가항목, 방법 등에서 큰 차이를 보이지 않아 이에 대한 검토 또한 필요한 실정이다.

본 논문은 이러한 연구의 일환으로 현 콘크리트 교량의 성능을 평가하는 기준의 타당성을 분석하는 데 목적을 두고 있다. 이를 위해 콘크리트 교량의 성능평가를 위해 국내외에서 실용하고 있는 지침을 분석하였다. 한국의 《시설물 안전 및 유지관리 실시 세부지침》, 미국 American Association of State Highway and Transportation Officials(AASHTO)의 《AASHTO The Manual for Bridge Evaluation》, American Concrete Institute(ACI)의 기준인 《Code Requirements for Assessment, Repair, and Rehabilitation of Existing Concrete Structures (ACI 562-16)》, 영국의 《BD 21/01 The Assessment of Highway Bridges and Structures》 등을 검토하였다. 추가로 현행 기준으로 사용되고 있지 않으나 한국도로공사에서 개발한 신뢰도기반 내하력평가 기준인 《신뢰도기반 교량 안전성 평가 지침(안)》의 내용을 검토하였다.

그 결과, 국내 기준만 유일하게 필수 점검 항목을 규정하여 모든 항목에 대해 등급으로 평가를 하도록 하며 각 부재에 대해, 교량 전체에 대한 상태안전등급을 산정하도록 규정하고 있음을 확인하였다. 또한 내하력평가에 대해 과거 설계기준에 기반하여 국외 기준보다 큰 하중계수를 적용하고 있었으며 이에 따라 교량을 보수적으로 평가할 것으로 분석하였다. 국내기준에서만 유일하게 교량의 안전성 평가를 위해 차량재하시험을 규정하고 있는 점 또한 문제점으로 분석하였다.

도출한 문제점에 대한 검증을 위해 실제 사례를 통해 그 타당성을 분석하였다. 서울시 내 교량 및 고가도로에 대한 안전진단 보고서와 관련 자료를 수집하였고 각 사례에 대해 살펴본 국내외 지침에 따라 내하력 평가를 수행하였다. 차량재하시험에 대한 검토를 위해 한 사례 교량에 대해 실험을 수행하였다. 또한 수집한 보고서 내 재료시험 이력을 분석하였다. 내하력 평가 결과 현 국내 지침이 교량을 가장 보수적으로 평가하는 것을 확인하였다. 따라서 AASHTO, 한국도로공사 등의 신뢰도 기반 기준을 적용하는 것이 바람직할

것이다. 차량재하시험 결과를 분석한 결과, 교량의 강성변화를 차량재하시험을 통해 일관되게 평가할 수 없음을 확인하였다. 재료시험의 경우, 이력 분석을 통해 현 지침에 의해 비 일관된 평가가 도출됨을 확인하였고 이에 대한 개선방안을 제시하였다.

후속 연구에서 본 논문에서 도출한 문제점에 대해 실험적으로 검증하여 현 국내 콘크리트 교량 성능평가 지침을 개선할 수 있을 것으로 기대된다.

주요어: 콘크리트 교량, 성능평가, 안전성, 내하력평가, 차량재하시험, 재료시험, 유지관리, 열화

학번: 2017-29357